Hindawi
Geofluids
Volume 2023, Article ID 8040253, 25 pages
https://doi.org/10.1155/2023/8040253

Review Article

Mineral Crushing Methods for Noble Gas Analyses of Fluid Inclusions

C. Wilske, A. Suckow, C. Gerber, A. Deslandes, P. Crane, and D. Mallants

CSIRO Environment, Gate 5, Waite Rd., Urrbrae, SA 5064, Australia

Correspondence should be addressed to D. Mallants; dirk.mallants@csiro.au

Received 16 March 2023; Revised 22 May 2023; Accepted 25 May 2023; Published 14 June 2023

Academic Editor: Martina Zucchi

Noble gases are frequently probed for investigating fluid inclusions in minerals to unravel rock-forming processes through time. Over the last decades, heating and crushing have been the two main methods applied for noble gas extraction from fluid inclusions in ultrahigh vacuum (about 10^{-9} mBar). The heating of minerals or pieces of bulk rock causes the release of noble gases from both fluid inclusions and the mineral or rock matrix, the latter due to temperature-dependent mineral dehydration. Crushing of minerals only affects fluid inclusions and allows a release of noble gases at room temperature with minor contributions from the mineral matrix. This review describes different ultravacuum crushing techniques for noble gas analysis from fluid inclusions. It examines the technical details and operational conditions of each crushing system as well as methods to prepare samples prior to crushing. Crushing systems were found to have unique designs across the different laboratories reviewed; they include single or multiple sample loadings and manual, magnetic, or hydraulic operation of the crushing pistons. Due to the small amounts of noble gases released, the technology requires several mg to a few grams of rock material to achieve a measurement of all stable noble gas isotopes in a single fluid inclusion. While theoretically all stable noble gas isotopes are of interest, the elements and isotopes reported in different studies vary widely and reference materials as well as laboratory intercomparisons are lacking. The review includes applications on the origins of magmatic rocks and geochemical processes in the Earth's mantle, the origin and chemical composition of deep crustal fluids and how these contribute to the formation of minerals of economic interest, and paleoclimate studies based on speleothems.

1. Introduction

Fluids trapped as inclusions within minerals can be millions to billions of years old and maintain a record of the fluid composition (e.g., halogens, noble gases, CO_2, CH_4, H_2O, H_2S, and H_2) and environment at the time of mineral genesis (e.g., [1]). Such mineral fluid inclusions contain information about rock-forming processes through time and have been applied to study the genesis of ore deposits [2–6], mantle dynamics [7, 8], origin/features of extraterrestrial rocks [9, 10], surface processes [11], paleoclimate reconstruction [12–18], and deep groundwater circulation research such as in the Paris Basin [19, 20] or in the Permian crystalline basement of Canada [21]. Due to the growing need to also understand deep groundwater systems, their provenance and residence times, and how groundwaters have been interacting with mineral phases over time, an increasing number of studies aimed at characterizing the degree of isolation of aquifers from other reservoirs (e.g., for hydrocarbon production), for applications such as CO_2 geosequestration [22], waste disposal [23], or for tracing deep hydrogen and carbon cycles [24].

Noble gases enclosed in rock minerals provide important insights about different evolutionary stages of minerals or rock formations and of geological processes, such as pressure-temperature conditions during ore/rock formation, the nature, provenance, and evolutionary history as well as ages of geofluids [25]. ^{40}Ar-^{39}Ar chronology acts widely as a main application field (e.g., [26, 27]). The main noble gas isotope ratios used for the identification of fluid inclusion origins in rock material representative of different geoscientific study areas (e.g., "crustal rock studies," "mantle rock studies," "ore rock studies," extraterrestrial rock studies," or "deepwater studies") are shown in Figure 1. Particularly

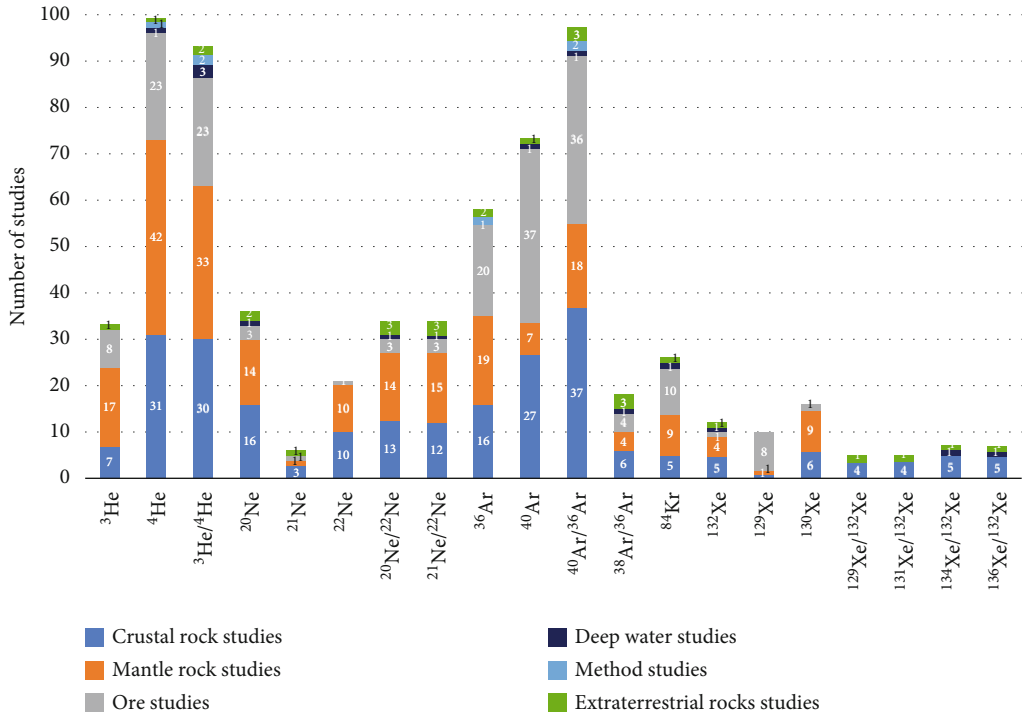

Figure 1: Commonly used noble gas isotopes and their geoscientific applications with an indication of a number of studies.

He isotope ratios have been successfully used in many studies, due to He isotopes being preferentially measured in the earlier studies with the available analytical set-up. As a result, He isotope systematics are relatively well understood and have been described in many studies [28–30]. The combination of noble gas analysis and halogens of irradiated samples has been successful in studying ^{40}Ar/^{39}Ar age systematics [31]. Analysis of halogens (Cl, Br, I) in fluid inclusions can be also accomplished by measuring irradiation-produced stable noble gas isotopes. The method is based on sample irradiation and neutron activation of halogens that produce noble gas isotopes such as ^{38}ArCl, ^{80}KrBr, ^{128}XeI, or ^{39}ArK as proxy isotopes for ^{40}Ar-^{39}Ar dating [32]. The main ultravacuum crushing method is made up of a Nupro valve type crusher (screw-type crushing systems) for noble gas analysis for ^{40}Ar-^{39}Ar dating and is often combined with heating experiments. The different crushing systems used in relation to the above-mentioned applications are summarized in Figure 2.

Fundamental for all applications of noble gas investigations in minerals and rocks is the knowledge about the characteristics of mineral fluid inclusions, and their geological context and how diffusion of noble gases within and between mineral phases occurs. Diffusion in minerals may occur within large mineral grains, along fast pathways (fractures), along the crystal lattice by Fickian diffusion [33, 34], and along intracrystalline defects such as dislocations [35]. Different noble gases exhibited different time scales of migration via these different pathways owing to the difference in noble gas atomic size. For instance, ^{40}Ar has a lower diffusion coefficient in olivine (ca. 5×10^{-13}m^2/s at 673-1673°C [36]) compared to ^{3}He (ca. 5.55×10^{-7}m^2/s at 553-893°C, [37]) due to the higher atomic size of argon (Ar: 4.86×10^{-10} m atomic size [38]) compared to helium (He: 2.88×10^{-10} m atomic size [38]).

The different diffusion rates of the noble gases can be used for characterizing different features of rocks and minerals. For instance, the modelling of ^{4}He diffusion between pore-water and quartz has been used to infer the permeability of sedimentary rock formations with excellent sealing capacity [39]. Heavy noble gases like Ar and Xe have been studied to understand the original composition of the fluid inclusions [31]. Ratios of radiogenic (e.g., ^{4}He) and primordial (e.g., ^{3}He) isotopes of noble gases can further identify the mixing of mantle, crustal, atmospheric, or solar system endmembers in fluid inclusions. In this regard, Ne isotopes have been applied for clarifying the origin and evolution of minerals and rocks [40, 41]. Argon has been used for differentiating between atmospheric and mantle fluid origins as well as obtaining age information or halogen content [30], while Xe isotope patterns have been applied to identify very old fluids from mines several km deep [42].

Heating and mechanical crushing are the two most common approaches to extracting fluid inclusions from mineral grains for noble gas analysis. Less common is the extraction of noble gases by laser ablation. In comparison to heating, crushing is less efficient in breaking all fluid inclusions [43]. Heating of whole rock or mineral samples is generally applied until melting of the sample results in the release of gases from the rock/mineral matrix. A stepwise increase in the temperature may be used to release different generations of fluid inclusions. A detailed discussion on the performance of stepwise crushing is provided in Section 4.3. However, advantages of crushing measurements include lower blanks

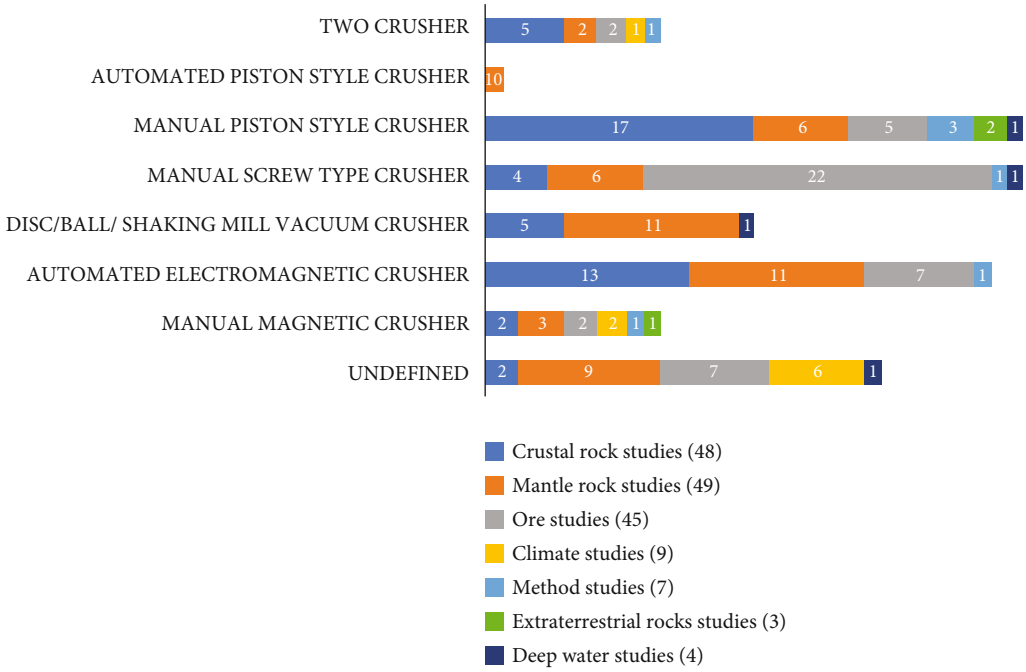

Figure 2: Overview of crusher types used in different studies (total number of studies are indicated).

(i.e., lower background concentration) of the crushing apparatus, e.g., 10-100 times lower, and there are also less issues with in situ produced isotopes and adsorbed atmospheric gases [43, 44]. Heat may be applied to release fluid inclusions from shungite to study argon isotopes for age estimations [45]. The limitation of the heating technique is that it may induce noble gas fractionation and/or promote the diffusion of noble gases from within the mineral matrix, therefore complicating the analysis.

Several studies have combined both crushing and heating to compare the noble gas composition of the matrix and the fluid inclusions [7, 32, 46–53] or to minimize diffusive gas loss from the small grains to ensure quantitative water extraction [15]. Further on, for He, crushing is supposed to be the prime method to extract mainly the magmatic He and less the in situ produced and cosmogenic He located in the crystal matrix [54]. Some minerals are unstable above ca. 800°C as, e.g., dolomite. Therefore, vacuum crushing is preferred over heating for noble gas extraction from fluid inclusions for most applications [55].

This paper reviews mineral crushing techniques for subsequent noble gas isotope analysis and their specific applications. The review focuses on mechanical crushing in ultrahigh vacuum conditions only. The crushing methods examined include magnetic crushing, piston crushing, and milling/shaking crushing. This review covers crushing methods of whole rocks and separate minerals for noble gas analysis of fluid inclusions that have been applied for the last fifty years. Alongside the development of noble gas release methods, the decades of application in the geosciences have been enabled by advancements in the noble gas measurement systems, such as high resolution and high sensitivity multicollector systems with automated detector movements. We summarize sample description and provide measurement specifications, which have been used across different applications.

2. Fluid Inclusion Genesis

Fluid inclusions are trapped fluids in a mineral's crystal lattice, typically of heterogenous composition, often including gaseous, liquid, and solid phases [55]. The size of fluid inclusions varies from 1 nm [56] to tens to hundreds of micrometres but typically is no larger than a few millimetres [55]. According to the stage of crystal evolution, three different types of fluid inclusions are distinguishable (Figure 3): (i) fluid inclusions evolving during crystallization from melts (melt inclusions), (ii) fluids that are trapped in crystal overgrowths, and (iii) fluids that are trapped along a healing fracture zone within a crystal (secondary fluid inclusions) ([55, 57]). Primary inclusions is a term used for inclusions entrapped during and as a direct result of crystal growth. A fourth type are the so-called pseudo-secondary fluid inclusions: these can occur in mineral grains where mineral fractures originating from deformation processes have healed and included fluids present around the grains during the healing process [55]. Inclusions trapped during the growth of a mineral are most likely to be representative of the conditions that existed during mineral growth, while inclusions trapped after mineral growth are likely to record later, potentially different conditions. Unlike primary inclusions, the secondary ones contain fluids that existed at some time after the growth of the host crystal, possibly millions of years later.

Noble gases are investigated in fluid inclusions occurring in a variety of minerals, e.g., in olivine, pyroxene, amphibole, sulphides, or basaltic glasses; these are of interest when questions about magma origins and mantle contributions are

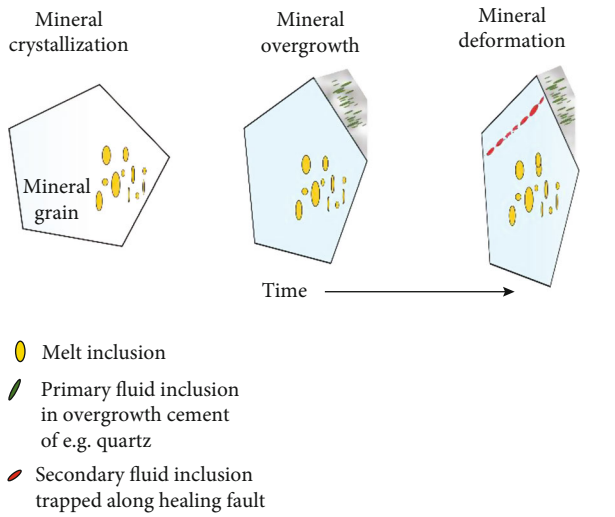

Figure 3: Cartoon with different types of fluid inclusion (modified after [55, 57]). During mineral crystallization from magma melt, inclusions are trapped as remnants from the melt in the crystal (yellow bubbles). Mineral overgrowth (greyish area on the mineral surface) occurs on crystal surfaces and can trap fluids during growth (green bubbles). When minerals are deformed during, e.g., tectonic stress, existing fractures can be healed with fluids (red bubbles).

investigated. Studies of crustal composition and origin have analysed fluid inclusions found in olivine, calcite, fluorite, eclogite, corundum, quartz, or whole rock pieces (e.g., [58–61]). Common minerals relevant for noble gas analyses in fluid inclusions for ore studies are ore-associated minerals like quartz, pyrite, calcite, or fluorite (e.g., [3, 40, 53, 62]). Palaeoclimate focussed studies have relied on noble gases in cave rocks like stalagmites (e.g., [12, 14, 17]). Meteorites or lunar rocks have also been investigated using noble gases in fluid inclusions for, e.g., investigation of ancient atmospheric composition (e.g., [9, 10]).

Mineral or rock selection is therefore based on the availability of types of minerals in the geological environment being studied, but the selection also depends on how the noble gases are trapped in the minerals. Noble gases can be entrapped in the fluid inclusions during crystal growth (melt inclusion or primary inclusions) or in healed fractures (secondary fluid inclusions). Three processes for modifications of the original composition of noble gases in the fluid inclusions postentrapment have been described [31]: (i) by cosmogenic production in rocks exposed to the Earth surface, (ii) from the production of radiogenic noble gas isotopes from the decay of naturally occurring U, Th, or K, or (iii) from postentrapment leakage of helium via diffusion. Therefore, inferences on when and how the noble gases are trapped in the fluid can be derived from analysing the mineral fractions containing a single type of fluid inclusion or by sequential analyses (e.g., multiple crushing steps) of complex minerals. The key processes resulting in changes to noble gas composition are further discussed based on grouping from [31].

Cosmogenic production of rocks exposed to the Earth surface is important for ^{3}He and ^{21}Ne in terrestrial samples [11, 63–66]. The principle is based on cosmic ray-induced in situ production of nuclides in rocks (and their fluid inclusions) exposed at the Earth's surface and has been used to study erosion of rocks (e.g., [11]).

The radioactive decay of naturally occurring ^{238}U and ^{232}Th in minerals produces ^{4}He, while ^{40}Ar is produced from the radioactive decay of ^{40}K. U, Th, and K can be found in the mineral matrix or within minor impurities [31]. Minerals with low U, Th, and K contents like quartz, calcite, olivine, or sulphide contain negligible radiogenically produced ^{4}He and ^{40}Ar [31]. ^{3}He can be produced in situ by neutron capture by Li, for example, in Li-rich fluid inclusions in combination with neutron supply of U-rich host rocks [67]. This can be significant for fluid inclusions with low He, because production of ^{3}He is very small, only, e.g., <10 ^{3}He atoms $g^{-1}a^{-1}$ in fluid inclusions where the rocks contain ca. 50 ppm Li and 10 ppm U [31, 67].

Leakage of noble gases is not uncommon in quartz crystals where anomalously low He/Ar ratios indicate a loss of He [31, 68, 69] or a difference in the age between fluid inclusion and rock [70]. Heavier noble gases (Ne, Ar, Kr, and Xe) are less diffusive and are less susceptible to being lost from the fluid inclusion after entrapment ([68, 69]). Many of the minerals which keep helium over geological time scales (10^{7}-10^{9} years [31, 33]) are dense minerals like pyrite or arsenopyrite. This group of minerals is referred to as opaque minerals, which makes fluid inclusion studies by standard microscopy difficult. It has been argued that there are no petrographic characteristics for selecting minerals with high helium retention, where helium retention is possibly a measure of individual lattice dislocations intersecting fluid inclusions [31]. However, magnetite, fluorite, scheelite, sphalerite, chalcopyrite, and native gold are considered helium retentive [69, 71–75]. Identification of any He loss in fluid inclusions is possible via analysis of all noble gasses and a comparison of the isotopic ratios against crustal production ratios, atmospheric ratios, mantle ratios, or solar system ratios.

3. Mineral Crushing Methods

Dependent on the intended geoscientific or industrial applications of fluid inclusion investigations, different types of crushing systems under vacuum have been used. Broadly three types are distinguished: (i) (electro) magnetic crushing, (ii) crushing by milling/shaking, and (iii) piston crushing (Figure 4). Each type can be further subdivided according to pressure strength, the degree of crushing automation, and whether single or multiple crushing containers are used.

3.1. Magnetic Crushing Systems

3.1.1. Manual Systems. The set-up of a magnetic crushing system consists generally of a stainless-steel tube (bottom closed) which keeps the sample at the bottom of the tube; a rod or ball inside the tube is moved magnetically in a manual way to crush the sample. These crushing systems are equipped with a 10 cm long tube connected to the measurement line and a pestle weight of 500 g to crush the sample with 50 steps [53]. Some systems use a 3 cm deep cylindrical

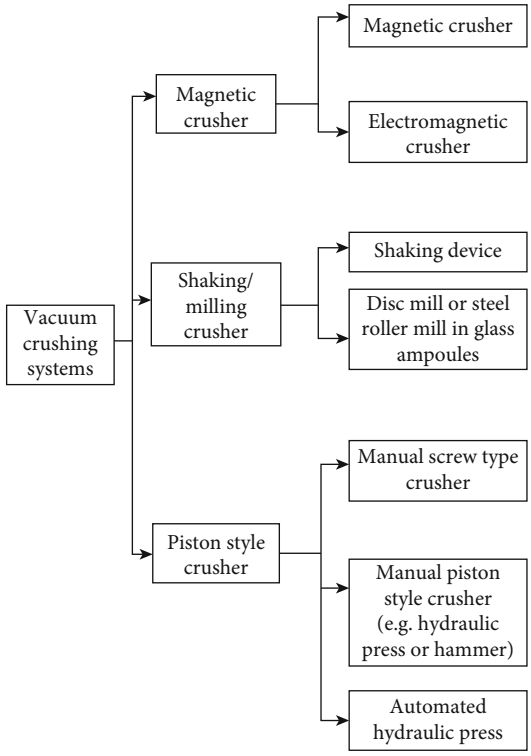

Figure 4: Classification of different vacuum crushing systems.

stainless-steel cup, placed into the crusher covered with a 9 mm diameter disc [76].

For soft materials such as carbonate rocks from speleothems, rock fragments are crushed with a stainless-steel ball lifted manually with a magnet along a long slim vertical crushing container [14]. The sample container is directly connected to the noble gas mass spectrometer (MS) and sample preparation line (Figure 5).

Other crushing systems consist of 3 high-vacuum, non-magnetic tubes connected to a noble gas MS with the capacity to crush 3 samples in a row [77]. A metal ball in each tube is operated manually with the use of a permanent magnet to crush the ≤3 g sample in a stepwise manner. The magnetic crusher is also applied at other institutes (see Table 1) to analyse noble gases in mantle rocks including the minerals olivine and pyroxene [78, 79]. This crushing system allows the application of multiple crushing steps ranging from 50 to a few thousand accumulated crushing steps. Mineral grain sizes range from 0.5 to 1.5 mm for quartz and fluorite, 2 to 3 mm for calcite and fluorite, and <10 mm for olive-containing xenoliths (Table 1).

3.1.2. Electromagnetic Systems. Electromagnetic vacuum crushing systems are in use for both soft and hard minerals and operate while fully connected to the measurement device (Table 2). It involves moving a nickel bolt up and down a cylindric crusher container in a magnetic field. Examples of this system can be found at the University of Oxford where ca. 2 g of sample material are crushed with an electromagnetically lifted nickel bolt with adjustable frequency (personal communication Dr. Rosie Jones, University of Oxford) (Figure 6).

Modifications of this set up include the use of a tungsten carbide piston with a nickel guide [84]. The magnetic field is induced in three water-cooled solenoid coils attached to the crusher container creating an operating current of 30 amperes with ca. 300 strokes/min of the piston [84]. Before starting the experiments, this crusher is operated sample-free for ca. 30 min [84]. A modification of this device was used in [85], which includes the possibility to separate the solenoid coils from the crushing device thus allowing to connect numerous crushers for running multiple crush experiments.

Another modification was introduced by [47], who used a stainless-steel electromagnetic crusher with a crushing rod weight of 80 g and a crushing tube of 20 cm height.

Further details about the operating parameters of an electromagnetic crusher can be found in [86]. Their five computer-controlled solenoids operate in sequence to lift the magnetic crushing rod with a frequency of 1 stroke/2 sec and an energy impact release of ca. 0.4 Joule/stroke. The duration of each crushing cycle and the number of crushing steps can be adjusted to the requirements of the experiment. Crushing steps up to 100-300 strokes were used on 0.5 g of basalt samples ([7]). Multiple crushing steps were also used by [87] to maximise the release of noble gases.

The number of steps may be adjusted depending on the mineral type, e.g., for carbonates a sequence of three steps with 15, 300, and +300 strokes were used while for apatite 15, 500 and +500 strokes were used [88]. The first step is typically applied to release the gases from the larger inclusions with possibly a larger fraction of atmospheric gases; the second step delivers the main extraction while completion is achieved in the third step.

Crushing experiments have been performed by activating the bolt for 3 to 8 min (ca. 60 drops/min) with sample amounts not more than 700 mg [54]. Higher sample amounts were shown to become compacted while crushing, rendering the experiment less reliable. This is due to the dimension of the crusher; a larger sample amount would compact easier with the less efficient crushing of the grains as only part of the grains is able to get crushed in the confined space of the crusher. Using a smaller amount of sample provides more space to crush grains owing to the larger space between the grains.

3.2. Milling and Shaking Crushing Systems. Several off-line high-vacuum crushing systems have been developed over the years, often based on the principle of crushing rock or mineral samples in sealed glass (Table 3). The design used by [70, 95] is based on a steel roller mill with 3 mm diameter iron balls or a disc mill. Generally, the glass ampoules are sealed with the sample inside and steal rollers (6 mm length, 4 mm in diameter) or a disc mill to crush the sample by vibration and rotation [70, 96] for between 20 to 30 minutes [70, 97].

The shaking-based systems require a stainless-steel container, a crush rod, and two high-vacuum, all-metal valves. The system is operated by shaking the unit for less than 5 minutes for quartz mineral grains [60]. Mineral fragments of 0.7 to 3.1 g can produce a grain size of 0.5 to 1 mm after crushing [60].

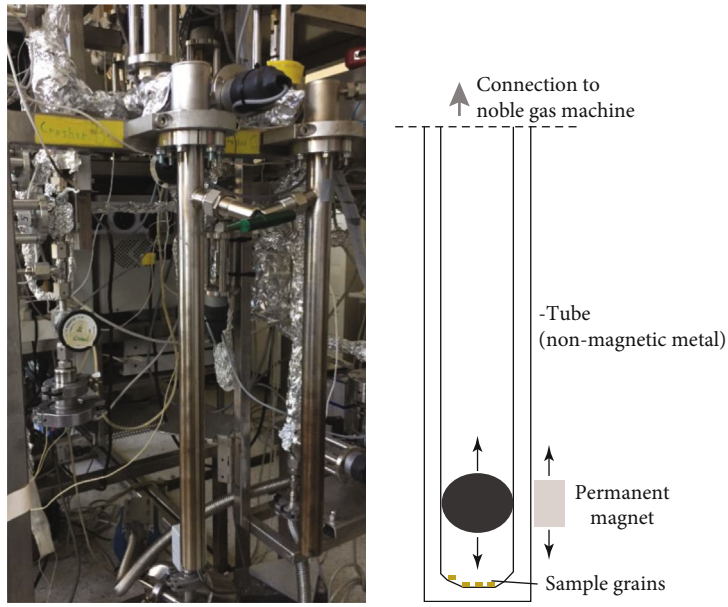

Figure 5: Manual magnetic high-vacuum crushing system at the University of Heidelberg. (a) Magnetic crusher and (b) Illustration of crusher and functionality.

3.3. Piston-Style Crushing Systems

3.3.1. Hydraulic Press Systems. Piston-style crushers are connected to a hydraulic press to crush in manual or automated mode (for a summary of studies, see Table 4). They have been applied to various minerals, including olivine, pyrite, quartz, or sedimentary rocks. At the University of Oxford (Figure 7 and Table 4), the system consists of one stainless steel sample container and 2 sets of tungsten carbide sample plates for processing 1 g samples in between each plate pair (personal communication Dr. Rosie Jones, University of Oxford). The crusher is driven by a manual 10 ton press (ca. 1544 bar), and it is noted that 8 tons (ca. 1235 bar) is generally sufficient to crush most minerals. While crushing, the system is permanently connected to the measurement unit. A similar experimental setup was reported by [85], who used pressures up to 700 bar delivered by a hand pump.

The crusher systems reported by [95, 98, 99] are all variations of the same basic design, with differences in maximum applicable pressure (Table 4). For example, one crusher uses a stainless-steel system connected to an automated hydraulic press with adjustable pressures up to 200 bar [95]. The sample container can be filled with ca. 1 g sample material of similar grain size between 0.5 and 2 mm, with pressures applied vertically via a piston. Another crusher uses single-step systems with a stainless-steel bowl in ultrahigh vacuum conditions which can apply up to 2000 bar pressure [98]. This crushing system is capable to process six samples simultaneously [61, 100, 101]. [99, 102] used a combination of a 1 cm diameter and a 6 to 10 cm long stainless-steel sampler, a hydraulic piston with applied pressure up to 200 bar, and a stainless-steel plate (AISI 316 LRN) placed below the sampler. Flexible stainless-steel tubes, heated to about 200°C with heater tape to prevent gas adsorption and improve gas flow in the system, connected the sample holder with the purification line. Purification steps were build-in to separate the CO_2 from the He fraction in a glass sampler; the He trapped in the glass sampler was transferred to a mass spectrometer for measurement. A single-step crushing device that uses a hydraulic press to crush samples placed in an aluminium holder separated by an aluminium plate at about 138 bar pressure was reported by [103, 104].

One of only a few automated hydraulic press systems was reported by [115]. The automated press operates with a sample chamber which includes 6 stainless steel sample containers, each with their own little hammer (Figure 8). In any given measurement sequence, one sample container is used as a blank sample. The automated system is connected to a piston, which can be moved via a turn table to the sample container with the hammer to crush a sample amount of 0.4-0.7 g. Depending on the mineral hardness, crushing steps will be adapted, e.g., using 300, 500, or 800 steps.

3.3.2. Screw-Type Crusher. Manually driven screw-type stainless-steel crushers with a single sample chamber have been used for both hard and soft rocks [9, 11] (Figure 9 and Table 5). These systems use a single piston which can be rotated ([9]) or pressed ([11]) to crush the samples. In [9], the crusher has a set of modified high-vacuum angle valves (CF16 flanges) and a rotation system inside for manually adjusting the piston up and down. This allows for controlling the crushing intensities, particularly for softer samples. Multiple crushing steps consist of slowly pressing first until the first cracks appear, then repeating the crushing until the cracking sound of the sample has stopped [9]. The first crushing step delivers most of the gases, i.e., primarily

Table 1: Fluid inclusion studies based on manual magnetic crushers.

Mineral/rock type	Sample preparation steps	Sample amount (g)	Grain size (mm)	Crushing steps	Reference
Speleothems	Evacuation in crusher container for 8 h, 70°C	—	—	60 steps	[14]
Calcite (1), siderite (1), dolomite (1), olivine (3), pyroxene (1, 2, 3)	Mineral preparation includes handpicking, washing of sample with ethanol ultrasonically, drying for 2-3 h, evacuation of crusher container at 120°C (2, 3) or 120-150°C for 12-24 h (1)	<3 (1)	1 to several mm (2, 3)	300, 450, 700, 1000, 1500, 2300, 3300, 4800, 70000 (2, 3)	[45] (1), [78] (2), [80] (3)
Calcite, fluorite	Washing of sample with ethanol & acetone in ultrasonic bath, drying at 50°C; evacuation in crusher container at 150°C	0.6 to 2.9	2 to 3	—	[58]
Meteorite	Evacuation at 100°C (ca. 3 weeks)	—	—	—	[10]
Olivine, dunite, basaltic glass	Mineral preparation includes handpicking, washing of sample in double-distilled water, ethanol, and acetone ultrasonically, evacuation of crusher container at 120°C for 10 h	1 to 3	≤10	—	[79]
Quartz	Mineral preparation includes rock grinding, sieving, electromagnetic separation, mineral handpicking	—	0.5 to 1.5	50 steps	[53]
Quartz, fluorite	Mineral preparation includes rock grinding, sieving, mineral handpicking, washing of sample in methanol ultrasonically	—	0.5 to 1.5	—	[76]
Eclogite (3), peridotite (1), xenolith (1), pyroxene (1, 2), clinopyroxene, basaltic glasses (4), dunites (5), xenoliths (6)	Mineral preparation includes sieving and handpicking (3, 4), washing of sample with ethanol ultrasonically, drying for 2-3 h, evacuation of crusher container at 120°C (4)	1.9 to 11.1 (1); 4.6 to 5.6 (2); 0.3 to 5.6 (3); 1 to 2	>0.315 (3); 1 to a few mm (4)	Three crusher tubes; stepwise crushing (e.g., 200, 1000, 3000) (1, 3); stepwise crushing 6, 200, 1000, 2600 strokes (4), up to 600 (5)	[81] (1), [82] (2), [59] (3), [80] (4), [8, 83] (5)
MORB glass	Washing of sample with HF, evacuation at 100°C for 24 h	1.3 to 2.3	—	50 to 100 strokes stepwise	[46]

A stroke means a single application of pressure onto the sample. Several strokes can be combined into a step, and subsequent steps can have different numbers of strokes each.

Table 2: Fluid inclusion studies based on electromagnetic crushers.

Sample type	Sample preparation steps	Sample amount (g)	Grain size (mm)	Crushing steps	Reference
Basalt, dolerite, gabbro	Washing of sample with ethanol or acetone (1), with acetone and deionized water ultrasonically (2), evacuation in crusher container for 12-24 h, 120-150°C (1,2) plus further 48 h pumping (1)	0.5 (1,2); 1 (3)	—	2000 strokes in a single step (1,3); 100 to 300 strokes in 3 to 6 crushing steps (2)	[7] (two crusher: Tokyo (1), Manchester (2)), [85] (3)
Quartz, sulphides	Mineral preparation includes mineral handpicking, washing with deionized water, acetone ultrasonically, evacuation at 125°C overnight	0.2 to 0.9	0.5 to 1	—	[89]
Mylonite	Mineral preparation includes the coarse crushing, handpicking, washing with distilled water, acetone ultrasonically, evacuation at 120°C overnight	0.22	1 to 3	20 to 40 strokes	[90]
Olivine, pyroxene	Mineral preparation includes handpicking, washing with deionized water (20 min), acetone (5 min), evacuation at 200°C for 24 h	1	1 to 2	e.g., 4 steps of 100, 200, 500, and 1000 strokes	[87]
Olivine (1), clinopyroxene (1), amphibole (2)	Mineral preparation includes handpicking (1), washing with distilled water and ethanol ultrasonically (1), evacuation until 10^{-7} torr (1) or with the sample at 200°C overnight (2)	1 to 3 (1)	0.4 to 2 (1)	Stepwise, e.g., for 0.5, 1, 3, 5, 15.5, 15 min (stroke every 2 seconds) (1)	[86] (1), [47] (2)
Pyroxene, olivine	Washing with distilled water ultrasonically, evacuation overnight	2	—	Crushed under vacuum for 2.5 min	[91]
Quartz, sphalerite, galena, pyrite, enargite	Mineral preparation includes rock grinding, sieving, mineral handpicking, washing of sample with HF or aqua regia, distilled water, methanol, evacuation in a crusher container overnight at room temperature	1 to 3	—	10 min	[40]
MORB (1, 2), xenolith (3)	Mineral preparation includes crushing, sieving, magnetic separation (3) mineral handpicking (1, 3), washing of sample with ethanol, and acetone ultrasonically (1, 3)	0.2 to 0.3 (1); 0.1 to 0.2 (2), 0.2 to 0.5 (3)	Several mm (2), 0.212-0.750 (3)	75 strokes (1)	[92] (1), [48] (2), [93] (3)
Carbonatite, apatite	Evacuation of crusher container at 150°C overnight	ca. 1	—	3 steps of 15, 300 + 300 strokes for carbonates, and 15, 500 + 500 strokes for apatite	[88]
Peridotite, olivine (1, 2), amphibole (2)	Mineral preparation includes heavy liquid separation and mineral handpicking, washing with 7% HF, distilled water, acetone, and ethanol (ultrasonically for 30 min) (1, 2)	1 to 2 (1)	1 to 2.4 (1, 2)	Crushing steps, e.g., 600, 900, 1100, 1800, whole rock and mineral (1, 2)	[84] (1), [94] (2)
Xenolith	—	≤0.7	—	3-8 min (60drops/min)	[54]

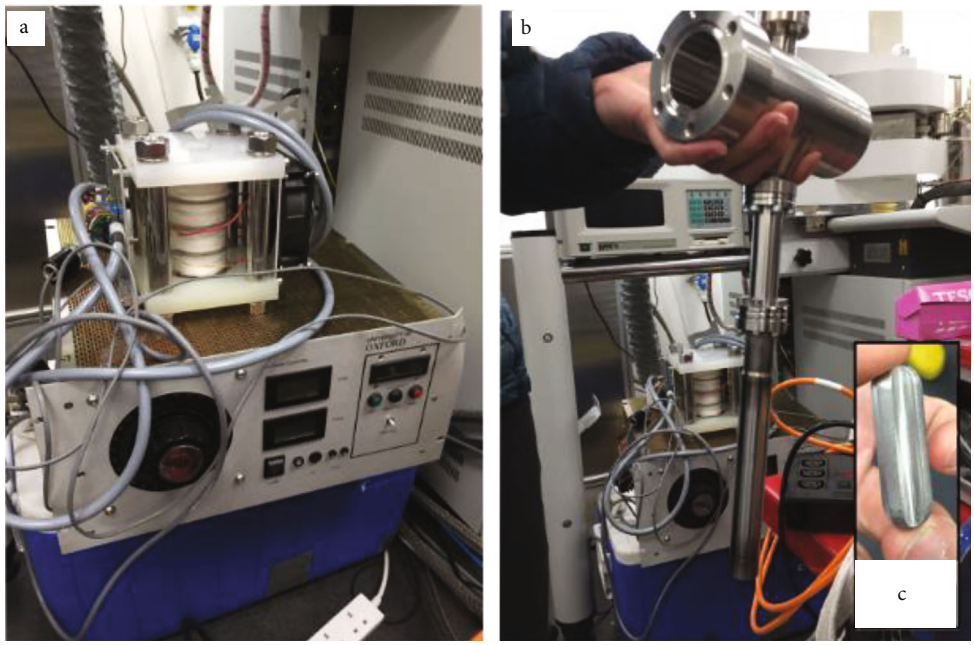

Figure 6: Electromagnetic crusher (a), an automatic-driven system with one crusher container (b), and a nickel bolt (c) at the University of Oxford.

Table 3: Fluid inclusion studies based on milling and shaking vacuum crushers.

Crusher type	Sample type	Sample preparation steps	Sample amount (g)	Grain size (mm)	Crushing steps	Reference
Shaking device	Quartz, calcite, barite	Mineral preparation includes separation of mineral grains, mineral handpicking, washing with water, ethyl-alcohol ultrasonically, evacuation at 100-150°C for several hours	0.7 to 3.1	0.5 to 1	<5 min	[60]
Glass ampoule together with a steel roller mill or disc mill	Nepheline, feldspar, apatite, pyroxene	—	1.5 to 2	0.25 to 0.6	Vibrational crushing	[96]
	Amphibole	—	—	—	20 min vibrational crushing	[97]
	Olivine	—	ca. 1	—	30 min vibrational crushing	[70]
	Amphibole	—	—	ca. 1	—	[47]

those residing within vesicles. The contribution of gases from the matrix is only obtained by applying another method, i.e. using CO_2 laser heating extraction.

With screw-type crushers, the pressure to crush can be increased in a stepwise fashion to crack the fluid inclusions. Some screw-type crushers have the capability to remove samples from the base plate without venting the system (Figure 9) and with the attachment of a PYREX™ sample carrier that can load up to 6 samples [116]. Special alloys are used for the front part of the piston like W-T-Co alloy to avoid cracking of the piston by the sample [117].

Sample amounts used vary from 0.4 to 0.7 g [9] to 1 to 1.5 g [11]. The crushing efficiency of an ultravacuum piston crusher is managed by a cylinder container instead of using bellows; this way samples of up to 1 g (2-3 mm grains) can be placed on a stainless-steel disc [118–120].

Modified Nupro valves® (Figure 10 and Table 5) are applied in several studies for crushing minerals. [122], for instance, used a manually driven crushing system consisting of sample chambers as part of the bottom part of the Nupro valves®, whereas the upper part includes the manually driven piston. Advantages of this type of crusher include the ability to crush up to 5 samples consecutively without opening the system (independent of mineral hardness), and more crucibles can be added for individual experiments. Rocks or minerals are crushed that vary in size from a single grain (e.g., [28]) up to a sample size of 1 g (e.g., [3, 4]).

4. Crusher Performance

The performance of crushers can be expressed in several ways. Here, we distinguish (1) crushing efficiency, (2) blank

Table 4: Fluid inclusion studies based on piston-style crushers.

Sample type He, Ne, and Ar in fluid inclusions from host to corundum rocks gneisses and mafic rocks with ultralight oxygen (Northern Karelia): isotope fractionation in an endogenic fluid	Sample preparation steps	Sample amount (g)	Grain size (mm)	Crushing steps	Reference
Sedimentary rock cores—quartz	Washing of isolated grains with acetone ultrasonically, evacuation at 150°C overnight	0.2 to 0.8	1 to 2	300 strokes	[49]
Travertine (1), olivine (2, 3), pyroxene (2)	Mineral preparation includes rock grinding, sieving, mineral handpicking (2, 3), washing with 6.5% HNO_3, deionized water (both ultrasonically) (2)	0.2 to 5.2 (1). 0.02 to 1 (2), 0.1 to 1.9 (3)	>1 (1), >0.5 (2), 0.5 to 1 (3)	200 bar (1, 2, 3)	[61] (1), [105] (2), [100] (3)
Olivine (1,2), pyroxene (1,2)	Mineral preparation includes rock grinding, sieving, mineral handpicking, washing with 6.5% HNO_3 ultrasonically, deionized water	0.1 to 3.2 (1); 0.3 to 1.2 (2)	>0.5 (2)	200 bar, single step (2)	[106] (1), [99] (2), [102]
Olivine, pyroxene (1, 2)	Mineral preparation includes handpicking (1, 2), washing with 6% HNO_3, deionized water (1) or with 5% HNO_3, distilled water, acetone (all ultrasonically, 15 min) (2), evacuation at 130°C for 48-72 h (1, 2)	1.0 to 2.2	>0.5	200 bar	[101] (1), [107] (2)
Olivine, pyroxene (1, 2)	Mineral preparation includes rock grinding, handpicking (2), washing in 5%HNO3 ultrasonically, distilled water, acetone, evacuation at 130°C overnight	1 (olivine), 2 (pyroxene)	0.5 (1)	200 bar (1); 2000 bar single step (2)	[108] (1), [98] (2), [95]
Peridotites, pyroxenites (1, 2); olivine, pyroxene (1,3); xenoliths (olivine, pyroxene, amphibole) (4)	Mineral preparation includes rock grinding, handpicking, washing with 6.5%HNO_3, deionized water ultrasonically, evacuation at 150-200°C (2,4)	2 g of Olivine (1), 0.5 to 1 g of pyroxenes (1); 0.3 to 0.6 (2); 0.2 to 1 (3); 0.03 to 1.1 (4)	>0.5 (4)	200 bar (1), 200 bar (2, 3, 4)	[109] (1), [110] (2), ([111] He, Ne, and Ar in fluid inclusions from host to corundum rocks gneisses and mafic rocks with ultralight oxygen (Northern Karelia): isotope fractionation in an endogenic fluid) (3), (4)
Pyrite	Mineral preparation includes rock grinding, washing with methanol, sieving, handpicking, distilled water	1	0.45 to 0.85	—	[112]
Scheelite, quartz	Mineral preparation includes rock grinding, handpicking	—	0.25 to 0.5	138 bar	[111]
Sulphides	Mineral preparation includes rock grinding, handpicking, washing with 5%HNO_3, deionized water, and acetone (all ultrasonically)	ca. 1	0.5 to 0.84	138 bar	[104]
Corundum, pyroxene, olivine	Mineral preparation includes rock grinding, sieving, handpicking, washing of sample with 5% HNO_3 for 20 min ultrasonically, distilled water	ca. 1	0.45 to 0.85	138 bar	[103]

Table 4: Continued.

Sample type He, Ne, and Ar in fluid inclusions from host to corundum rocks gneisses and mafic rocks with ultralight oxygen (Northern Karelia): isotope fractionation in an endogenic fluid	Sample preparation steps	Sample amount (g)	Grain size (mm)	Crushing steps	Reference
Quartz, Arsenopyrite, pyrite	Washing of sample with distilled water	0.5	0.4	138 bar, single step	[113]
Pyrite	Mineral preparation includes rock grinding, sieving, washing with distilled water, evacuation	0.5 to 1	0.45 to 0.3	Single step	[114]
Pyrite, chalcopyrite	Mineral preparation includes rock grinding, handpicking, washing with alcohol, evacuation at 120-150°C, for >24 h	0.1 to 1	>0.25	—	[6]
Olivine, pyroxene	—	3	—	700 bar	[85]
Olivine	Washing of samples includes leaching with 7%HF (10 min), 3× water, in an ultrasonic bath with acetone and ethanol (30 min), overnight drying (60°C)	1 to 2	—	100 bar, multiple steps	[115]

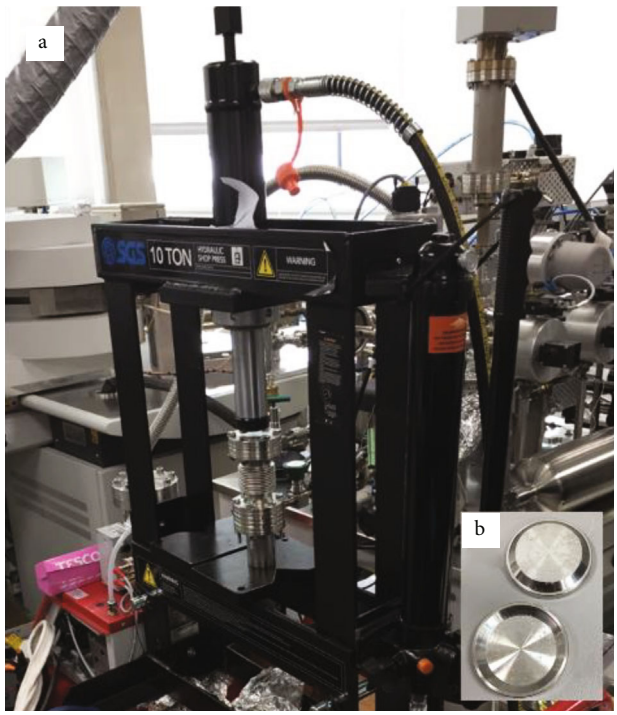

Figure 7: Hydraulic press (a) and stainless-steel sample plates (b) at the University of Oxford.

levels and noble gas adsorption to experimental equipment, (3) the number of crushing steps, and (4) sample preparation steps.

A comparison of features of the different crusher types discussed in previous sections is available in Table 6. Most of the crusher types are directly connected to the gas separation and measurement system ("online" crusher), whereas "offline" crushing systems are operated disconnected from the measurement system. The "offline" systems first collect their gases into containers like the stainless tubes of a magnetic crusher, stainless steel vessels of a shaking crusher, or milling crushers with glass ampoule crushers; subsequently, gases from the containers are released into the measurement system.

4.1. Crushing Efficiency. The noble gas concentrations obtained from crushing experiments may be influenced by the different sample manipulations such as further grain-size reduction due to chiselling out crushed samples from sample holders, aggregates lumping together and not passing a sieve, or loss of noble gases from rupturing of large (e.g., >75 μm) fluid inclusions [133, 137].

To check the efficiency of crushing, some studies have analysed grain size distributions after crushing (Table 6) resulting in values between <630 and <200 μm for speleothems [14], <1500 μm for xenoliths [87], <150 μm for olivines [85], and<149 μm for pyrite [6]. Others have continued the crushing until no audible crushing sound can be heard in an attempt to reach a maximum extent of crushing [104]; alternatively, crushing experiments can be applied multiple times for improved efficiency [135].

Efficiency testing of crushing by means of scanning microscope images and computer analysis to calculate the crushed size fractions was done by [70] for fractions between 0.01 and 1 mm applied by a glass ampoule crusher. Others used a Beckman Coulter laser diffraction size analyzer for analysing the grain size distribution after crushing [90].

Using different amounts of quartz in the crushing experiments of [125] did not influence efficiency as all tests showed the same fraction (i.e., 60%) of grains <90 μm. Contrasting results were reported by [54]: a larger amount of sample resulted in a lower efficiency caused by crushed fine grains compacting the sample in the crusher. The use of different crushers can influence efficiency, as was demonstrated by [90]: their piston-style crusher (with a modified ¾″ Varian vacuum valve) produced coarser powders compared to a magnetic crusher able to exert a greater force.

Primary fluid inclusions smaller than 5 μm may remain in crushed minerals when their size exceeds that of the inclusion; as a result, noble gases in such small inclusions may be underrepresented in the analysis. Note that inclusions may come in all sizes and shapes, but commonly, many inclusions in a sample may be smaller than a micrometer [138]. Furthermore, in most samples, the secondary inclusions are much more abundant than the primary inclusions [139], and, importantly, fluids from the secondary inclusions distributed along microcracks are readily extracted by crushing [140]. This points to one of the limitations of the mineral crushing technique compared to other techniques such as heating. Especially those crushing techniques that generate very large grain sizes (Table 6) result in low efficiency in liberating fluids from primary inclusions.

The choice between heating and crushing also depends on whether primary or secondary inclusions are the target. As primary and secondary fluid inclusions have different size distributions, crushing and/or heating methods that have a different size cut-off will result in different fractions of primary vs. secondary fluid inclusions. Unlike crushing, heating would provide results that are more easily comparable between different studies because it does less strongly discriminate between different sizes, i.e., one always gets the same mix between primary and secondary inclusions. To improve the intercomparison between fluid inclusion studies, we recommend that any crushing study reports at least a best estimate of the grain size after crushing (and ideally a distribution rather than a simple cut-off). An example of postcrushing particle size data is available from [141] who showed that crushing quartz grains by a total of 10,245 pestle drops resulted in 6% of grains <1 μm, 82% between 4 and 1 μm, and 12% of the grains were >4 μm. The smallest grains were approximately 50 nm in size. As most of the primary fluid inclusions were 5–20 μm, their crusher effectively extracted the majority of the fluid inclusions visible with an optical microscope.

4.2. Blank Levels and Adsorption. Blank levels refer not only to the crushing devices but also refer to the blank level of the noble gas mass spectrometer (Tables 7 and 8). Indeed, the adsorption of gases released from the crushing device show temperature and pressure-dependent adsorption onto

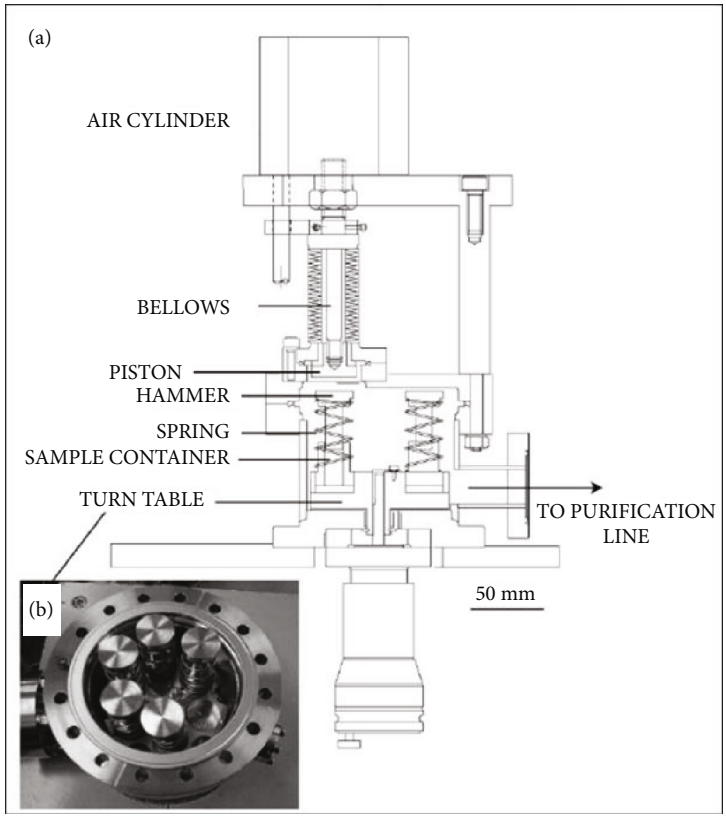

Figure 8: Automatic high vacuum crusher (online system) (a) with chamber and sample container (b) (reprinted from [115] with permission from Elsevier).

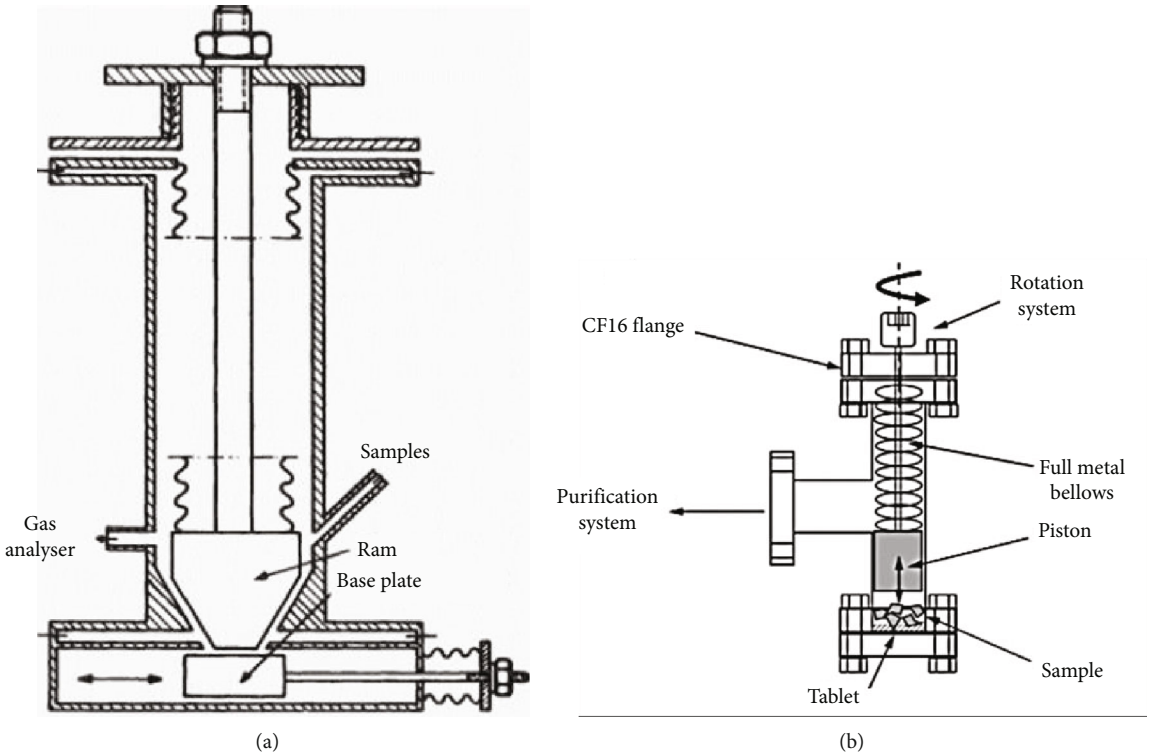

Figure 9: Sketch of screw-type crusher. (a) Manual high-vacuum crusher connected to noble gas MS (reproduced from [117, 121]. (b) Sketch of the manually driven crushing system [9] (reproduced from [9]) with permission from John Wiley and Sons).

Table 5: Fluid inclusion studies with modified Nupo valve crusher, screw-type crusher, and VAT valve crusher.

Crusher type	Sample type	Sample preparation steps	Sample amount (g)	Grain size (mm)	Crushing steps	Reference
Modified Nupro valve	Calcite, fluorite	Mineral preparation includes rock grinding, sieving, mineral handpicking, washing of sample with water (10 min), and acetone (20 min) ultrasonically	0.1	0.4 to 0.6	—	[62]
	Dolomite (1), quartz (2, 3)	Mineral preparation includes handpicking (1, 2), washing with distilled water, acetone ultrasonically (1, 2)	0.03 to 0.05 (1)	1 to 3 (1)	—	[123] (1); [124] (2); [125] (3)
	Quartz, fluorite	Mineral preparation includes rock grinding, sieving, mineral handpicking, washing with acetone before handpicking, evacuation at 200°C for 36 h	0.1	0.5 to 1	Crushed twice	[69]
	Pyrite (2, 4), pyrrhotite (2); scheelite (1, 3)	Mineral preparation includes sieving, mineral handpicking, washing of sample with distilled water, methanol ultrasonically, evacuation in a crusher container at 120-150°C (12-24 h) (1, 3), at 200°C for 24 (4) or 48 h (2)	0.2 to 1 (1); 0.3 to 0.5 (2); 0.2 (3); 0.01 to 0.2 (4)	1 to 5 (1); 0.5 to 2 (1); 0.5 to 1 (3); 2 to 3 (4)	—	For the above-mentioned main applications for noble gases in fluid inclusions, different crushing systems are used (Figure 10).
	Xenolith, amphibole, diopside	—	—	—	10 min each crushing step, 5 separate steps of increasing intensity	[126]
	For the above-mentioned main applications for noble gases in fluid inclusions, different crushing systems are used (Figure 10).	Evacuation at 150°C, >24 h	0.5	0.5 to 1.5	—	[127]
	Olivine, megacryst, picrite, tholleiite glass	—	0.25	0.1 to 0.5	—	[128]
	Pyrite (1, 2)	Washing of the sample with distilled water, and acetone ultrasonically, evacuation at 100-150°C for 24 h (1, 2)	1 (1)	0.2 to 0.8 (1,2)	—	[3] (1), [4] (2)
	Quartz, calcite	Mineral preparation includes mineral handpicking, evacuation at <150°C for >24 h	0.2 to 1	0.5 to 1	—	[129]
	Arsenopyrite (2), pyrite (1)	Mineral preparation includes grinding (1), mineral handpicking (1,2), washing of sample with alcohol, evacuation at 120°C for 6-8 h (1), at 150°C for >24 h (2)	0.2 (1); 0.5 to 1 (2)	>1 (1); 0.5 to 1.5 (2)	—	[29] (1); [130](2)
	Galena	Evacuation at 150°C, >24 h	0.5 to 1	1 to 2	—	[131]

Table 5: Continued.

Crusher type	Sample type	Sample preparation steps	Sample amount (g)	Grain size (mm)	Crushing steps	Reference
	Bornite, chalcopyrite	Mineral preparation includes rock grinding, sieving, handpicking, washing of sample with ethyl-alcohol in an ultrasonic bath, evacuation at 150°C (24 h)	1	0.25 to 1	—	[132]
Screw-type crusher	Lunar rocks, meteorites, terrestrial basalt	—	0.1 to 0.5	—	—	[121]
	Basalt (1), desert glass (2)	Mineral preparation includes handpicking after washing of sample with distilled water ultrasonically (1) or acetone and water ultrasonically (2), evacuation at 80°C overnight (1), at 120°C for 12 h (2)	0.17 to 0.37 (1); 0.05-0.1 (2)	1 to 2 (1)	—	[116] (1); [117] (2)
	Sphalerite, chalcopyrite	Evacuation in crusher container for 24 h, 100°C	0.67 to 2.15	—	—	[133]
	Quartz	Mineral preparation includes grinding, sieving to 500 μ to 1000 μm, washing with HCl at 80°C for 4-5 h, 3× leaching with HF/HNO_3 at 80°C for 5 to 10 h	1 to 1.5	—	—	[11]
VAT valve	Quartz (1, 2)	Mineral preparation includes rock grinding, washing with acetone ultrasonically, handpicking (1)	2 (1), 1 (2)	1 to 3 (1), 2 to 3 (2)	Up to 7 steps (2)	[118, 119] (1); (2)
	Basalt, lunar basalt	—	0.4 to 0.7	—	2 to 10	[9]
Spiral crusher	Pyrite, wolframite	Mineral preparation includes rock grinding, sieving, handpicking, washing with acetone ultrasonically, evacuation at 120-150°C	0.5 to1	>0.42	—	[134]

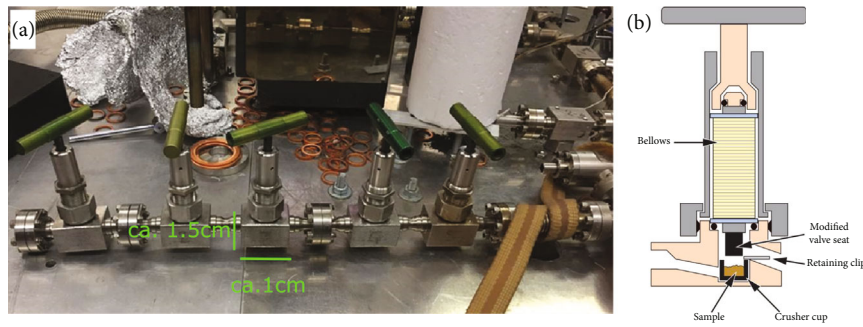

Figure 10: Modified Nupro® valve crusher type: (a) 5 Nupro® valve crusher in a row for crushing of 5 samples and (b) Schematic of Nupro® valve crusher, manual adjustable with bellows (modified from [44]).

Table 6: Comparison of features of different crusher types.

	Magnetic crusher		High vacuum crushing systems Shaking/milling crusher		Piston style crusher	
	Magnetic crusher (manual)	Electromagnetic crusher	Shaking device	Disc mill/ steel roller mill in glass ampoules	Screw-type crusher (manual)	Hydraulic press (manual/automated)
Offline/online crushing	Online/offline	Online	Offline	Offline	Online	Online
Multiple crusher container	1 to 3	No	—	—	Nupro valve crusher up to, e.g., 5	1 (manual)/6 (automated)
Crushing strokes	6 to 70,000	20 to 1800/ crushing for 2.5 to 10 min	Crushing for <5 min	Crushing for 20 to 30 min	Crushed twice (Nupro valve crusher), 2, 7, 10 (VAT valve crusher)	Single step 140 bar to 200 bar (manual), multiple at 100 bar (automated)
Sample amount (g	0.6 to 5.6	0.2 to 3	0.7 to 3	1 to 2	0.1 to 1	1 to 2
Sample size after crushing/ percentage of total amount/mineral	<630 μm/80%/ speleothems; <200 μm/40%/ speleothems [(1A)]	<150 μm/70-50%/ xenoliths[(2A)]	<120 μm/ 99%/basalt; <63 μm/70%/ basalt [(3A)]	<75 μm/40%/ xenoliths[(4A)]	50-100%/quartz, olivine[(5A)]	<149 μm/pyrite[(6A)]
		<150 μm/ 70%[(2B)]		10-15 μm/ corundum[(4B)]	60%/chalcopyrite; 20-12%/sphalerite, pyrite, marcasite[(5B)]	<25 μm/olivine, pyroxene[(6B)]
		A few μm/ amphibole[(2C)]		ca. 50 μm/ amphibole[(2C)]	<500 μm/60%/basalt; <50 μm/10%/ basalt[(5C)]	<75 μm/40%/ corundum, peridotite xenoliths[(6C)]
				1000-100 μm/ quartz[(4C)]	<75 μm/40%/ pyrite[(5D)]	<149 μm/ca. 30%/ sulphides minerals[(6D)]
					<100 μm/ scheelite[(5E)]	<150 μm/50%[(2B)]
					<100 μm/ca. 20%/ pyrite[(5F)]	

(1A) [14]. (2A) [84], (2B) [85], (2C) [47]. (3A) [135]. (4A) [96], (4B) (4C) [70]. (5A) [133], (5B) [136], (5C) [137], (5D) [43, 44, 127] (5E). (6A) [6, 114], (6B) [107], (6C) [103], (6D) [104].

components of the measurement device, which impacts the blank level and can influence the analysis of mobile noble gases or reactive gases like N_2, CO_2, or H_2O. The use of glass equipment in the extraction line of a mass spectrometer is less reliable for He analysis; Pyrex ® glass had higher He blanks in comparison to stainless steel, while Kovar ® glass had a 7 times smaller He blank caused by He diffusion through glass in comparison to Pyrex ® glass [79]. The ability for crushed minerals to adsorb gases is known to occur on basalt glass and quartz surfaces with the order of adsorption (strong to weak) $N_2<CH_4<CO<CO_2< H_2O$ [142], and on meteorites with stronger adsorption towards heavier noble gases leading to fractionation at low temperatures [143].

To avoid unwanted background levels of reactive gases, gentle crushing was shown to produce particularly low methane background levels in a steel crusher, while crushing laboratory glass allowed the detection of the background of adsorbed gases [121]. The background of adsorbed gases can

Table 7: Blank levels for system blanks He, Ne, and Ar isotopes.

Crusher	Study	He (cm^3 STP)	Ne (cm^3 STP)	Ar (cm^3 STP)
Magnetic crusher	[76]			$^{40}Ar\ 5\times10^{-10}$
	[77]	$^{4}He\ 3.2-5.6\times10^{-9}$	$^{20}Ne\ 1.2-4.3\times10^{-12}$	$^{36}Ar\ 0.8-7.2\times10^{-12}$
	[59]	$^{4}He\ 5.2-8.0\times10^{-9}$	$^{22}Ne\ 2.8-7.1\times10^{-13}$	$^{36}Ar\ 0.5-4.9\times10^{-12}$
	[93]	$^{3}He \le 1\times10^{-15}$ $^{4}He<1\times10^{-10}$		
Electromagnetic crusher	[84]	$^{4}He\ 2-4\times10^{-10}$	$^{20}Ne\ 7\times10^{-12}$	$^{40}Ar\ 2-20\times10^{-9}$
	[86]	$^{4}He\ 9.4\pm0.5\times10^{-8}$	$^{20}Ne\ 4.7\pm0.4\times10^{-11}$	$^{36}Ar\ 2.9\pm0.5\times10^{-12}$
	[85]	$^{4}He\ 2\times10^{-10}$		
	[88]	$^{4}He\ 20\times10^{-12}$	$^{20}Ne\ 4.4\times10^{-12}$	$^{36}Ar\ 0.8\times10^{-12}$
	[7]	$^{4}He\ 3.7\pm0.6\times10^{-11}$	$^{20}Ne\ 1.7\pm0.1\times10^{-12}$	$^{36}Ar\ 1.8\pm0.3\times10^{-12}$
Shaking crusher	[51, 135]	$^{4}He\ 5\pm2\times10^{-9}$		
Hydraulic press	[103]	$^{3}He<3\times10^{-17}$		
	[101, 146]	$^{4}He<10^{-9}$	$^{20}Ne<10^{-11}$	$^{40}Ar<10^{-9}$
	[111, 113]	$^{3}He\ 3\times10^{-17}$		$^{40}Ar<4\times10^{-11}$
Nupro valve crusher	[131]	$^{4}He\ 1\times10^{-11}$		
	[129, 130]	$^{4}He<2\times10^{-10}$		$^{40}Ar\ 2\text{ to }4\times10^{-10}$
	[11]		$^{20}Ne\ 0.5\times10^{-12}$	$^{40}Ar\ 0.05\times10^{-8}$
	[119]			

STP: standard temperature and pressure.

Table 8: Blank levels for system blanks Kr and Xe isotopes.

Crusher	Kr (cm^3 STP)	Xe (cm^3 STP)
Magnetic crusher	$^{84}Kr\ 3.8-9.7\times10^{-14}$	$^{132}Xe\ 3.0-9.1\times10^{-15}$
Electromagnetic crusher	$^{84}Kr\ 1-5\times10^{-13}$	$^{132}Xe\ 3-6\times10^{-14}$
	$^{84}Kr\ 4.7\pm0.9\times10^{-14}$	$^{130}Xe\ 0.73\pm0.15\times10^{-15}$
	$^{84}Kr\ 10^{-12}$	$^{132}Xe\ 0.3\times10^{-12}$
	$^{84}Kr\ 3.6\pm0.4\times10^{-14}$	$^{130}Xe\ 3.3\pm0.5\times10^{-16}$
Nupro valve crusher		$^{132}Xe\ 0.01\times10^{-12}$
		$^{132}Xe\ 10^{-13}$

STP = Standard Temperature and Pressure.

also be minimized in stainless steel crushers and its tubing by baking the crusher assembly up to 80°C [116] because gas desorption is promoted at higher temperature [118]. Using an electromagnetic crusher, no adsorption of CO_2 or CH_4 was detected when operating an empty device [142, 143].

Fluid inclusion-free samples have been used to determine active blanks [43, 69]. Using inclusion-free quartz resulted in ±50% error after repeated crushing experiments, not significantly higher than passive blanks from gas buildup during extraction and clean-up measurements with a screw-type crusher [43, 116]. Some types of crushers have been reported to result in low blanks, such as manual piston-style crushers in comparison with manual magnetic crushers, owing to the improved control of crushing and therefore softer crushing without wall grinding [120].

A limited comparison between electromagnetic and piston-style crushers has delivered some insights regarding their performance. [85] describes both crusher types: their hydraulic-type crusher uses up to 3 g of sample with an average grain size larger than 250 μm which is mechanically crushed using a hydraulic press of up to 70 MPa. This results in approximately 50% of the sample being crushed into powder with an average grain size of less than 150 μm. Their electromagnetic solenoid-type crusher can load up to 1 g of sample material into the crushing chamber; more than 70% of the sample is crushed into less than 150 μm after 1000-2000 strokes. Other differences between both crushing methods concern the blank levels of helium: these are 1×10^{-11} cm^3 STP for the hydraulic crusher and 2×10^{-10} cm^3 STP for the solenoid crusher. Regarding the fraction of noble

gases released, both systems seem to perform in a similar way. The electromagnetic crusher primarily releases noble gases from the microinclusions and minimizes release from matrix-hosted noble gases retained within solid phases [144]. Likewise, the piston-style system with single-step crushing also minimizes the release of matrix-sited noble gases [100]. Some vacuum crushers can produce very fine grains; e.g., for diamond crushing, the electromagnetic crusher was shown to produce very fine grains <100 nm, while some larger grains (up to 5 μm) [145].

4.3. Number of Crushing Steps. The application of multiple crushing steps to increase the efficiency of gas release has been applied in several studies for most crusher types. Initial crushes generally resulted in the highest volume of noble gases, with typically >80% of the helium being released by the application of an electromagnetic crushing device [54]. Especially stepwise release enables the stepwise extraction of noble gases and avoids the release of gases stored in the mineral matrix [78, 80]. It has been argued that extraction progresses from the largest to the smallest fluid inclusions and from dense fluid inclusion assemblages to less dense fluid inclusions [80]. Similar conclusions about the ability of stepwise crushing of magmatic minerals to release noble gases from two different gas reservoirs, i.e., primary (early release after ~0.5-~3 minutes) and secondary inclusions together with noble gases associated with the matrix (released after ~7–~13 minutes), can be found in [86].

The validity of the $^{40}Ar/^{39}Ar$ stepwise crushing technique for age dating of cassiterite and wolframite mineralisation was demonstrated by comparison with contemporaneous K-rich muscovite ages determined by $^{40}Ar/^{39}Ar$ laser stepwise heating [141]. The fluid inclusions in cassiterite and wolframite were extracted by stepwise crushing using a total of 18 steps, taking care of the number of pestle drops for each successive step increased to obtain argon levels conducive to precise measurements. The argon release pattern by progressive crushing revealed three broad types of argon reservoirs, similar to previous findings by [147]: (1) excess ^{40}Ar within secondary fluid inclusions typically distributed along cracks and therefore more easily extracted during the first couple of crushing steps (6 steps for cassiterite and 6-7 steps for wolframite); and (2) a mixture of radiogenic and trapped argon in small primary fluid inclusions and atmospheric argon from the crusher released during the final crushing steps. A third type contains a mixture of primary and secondary reservoirs. Importantly, all the cassiterite and wolframite samples dated by the stepwise crushing method resulted in isochron ages in agreement with those of the muscovite samples derived from laser stepwise heating. [141] suggest that the progressive crushing technique is suitable to directly determine the mineralisation ages of several ore-minerals, including cassiterite, wolframite, sphalerite, chalcopyrite, and pyrite, on the proviso that they contain sufficient primary fluid inclusions with adequate potassium concentrations (or salinity).

In [148], the gas release sequence from stepwise crushing of samples from granite and greisen (a highly altered granitic rock) was further refined by introducing six groups of gas reservoirs, here ordered according to increasing crushing steps: (1) microcracks with excess ^{40}Ar and an extremely low amount of potassium, (2) secondary inclusions with excess ^{40}Ar distributed along healed microcracks suitable for derivation of an inverse isochrone line typical of postmineralisation activities, (3) mixtures from the secondary and primary inclusions, (4) isolated, micrometer-sized primary inclusions suitable to derive an inverse isochron line for age dating of the primary mineralisation, (5) mixtures from secondary and primary inclusions representing a gas mixing line from fluids and solids, and (6) micro- to nanometer-sized solid minerals released by extended crushing. [149] commented that not all the above groups would necessarily be observed for any specific sample. The $^{40}Ar/^{39}Ar$ progressive crushing methodology resulted in primary inclusion isochron ages that agreed with the mica ages from laser step heating and cassiterite U-Pb ages using laser ablation-inductively coupled plasma-mass spectrometry. This demonstrates that the progressive crushing technique combined with multi-collector noble gas mass spectrometry of $^{40}Ar/^{39}Ar$ is a valid methodology to derive hydrothermal mineralization ages to date geologic events associated with K-bearing fluids.

4.4. Sample Preparation before Crushing. Sample preparation for noble gas extraction from fluid inclusions depends on the type of geological material that needs investigation: mineral veins, volcanic rocks, or sedimentary formations. The first step involves coarse crushing of the rock specimen followed by handpicking of minerals under a binocular microscope (e.g., [53, 62, 76, 120]). Prior to mineral selection under the microscope, crushed materials are sieved to a grain size fraction of 0.5-2 mm ([53, 76]) or >315 μm [59]. What minerals are selected depends on the type of fluid inclusions of interest; e.g., olivine is selected for their large fluid inclusions that are known to contain higher amounts of He [28].

A variety of chemical treatments exist to remove unwanted compounds from mineral surfaces. For instance, quartz clasts are leached with HCl at 80°C for 4-5 hours, followed by three leaching steps with HF/HNO_3 at 80°C for 5-10 hours in an ultrasonic bath for etching several micrometres of the quartz surfaces [11]. Megacrystal separates of volcanic rocks like corundum, titanomagnetite, pyroxenite, lherzolite, and wehrlite are cleaned with 5% HNO_3 ultrasonically for 20 min for removal of post eruption radiogenic components and then rinsed with distilled water and dried [103]. Olivine, amphibole, and whole rock separates are leached with 7% HF for 10 min and washed with distilled water [94].

Some of the unwanted compounds at the mineral surfaces include atmospheric gases. Desorption of such compounds may require distilled water and organic solvents like acetone ([3, 7, 62, 90, 120]), ethyl-alcohol [132], ethanol ([58, 94]), or methanol in an ultrasonic bath.

Removal of unwanted compounds from mineral surfaces can also be achieved by heating the samples when loaded in the crusher container, at which time also gases adsorbed onto the inside of the crusher equipment are also removed. Heating temperature and duration vary: 70°C for at least 8 hours for stalagmites [14], 100°C for 24 hours for sphalerite

[133], 100°C for 8 hours for fresh volcanic glass chips [120], 150°C for chalcopyrite, bornite, and galena [133], 150°C for 24 hours for basalts [7], and ca. 200°C for 48 hours for serpentine and chlorite [149].

5. Example Method Studies

Method studies involve a detailed investigation of fluid inclusions in different rocks or minerals, or they compare noble gases released from crushing or heating with the aim of assessing the quality of vacuum crushing for different mineral types. Manual piston-style crushers (partly with manual hydraulic press systems) were applied in some studies, while other studies used manual screw-type crusher, magnetic crusher, or electromagnetic crusher. Examples of method studies are briefly discussed.

Significant improvements in helium analysis may be obtained by applying a double collector system and two connectable crusher systems [85]. The combined system included a hydraulic press-type crusher and a solenoid crusher system connected to a high-vacuum heating system. All systems showed low He blanks and suitable natural samples with low noble gas concentrations or total gas amounts.

The effect of prolonged crushing on the validity and accuracy of helium concentrations and isotope ratios was demonstrated for magmatic crystals subjected to an electromagnetic crusher ([86]). Long crushing times revealed two exponential releases linked to two distinct gas reservoirs. Gases from the first reservoir were released during the first 0.5 to 3 min of crushing, while gases from the subsequent 7-13 min were linked to a secondary He reservoir. Because extended crushing may lead to a possible mix of released He from both primary and secondary inclusions or matrix-stored He, only the initial short-duration crushing steps should be considered to avoid such mixing.

To investigate irradiation-produced noble gas isotopes in scapolite and hydrothermal quartz, two crusher types, a Nupro valve crusher and a hydraulic press, were compared (e.g., [27]). Crushing the scapolite released ca. 4% of the irradiation-produced $^{38}Ar_{Cl}$ in comparison to 98% released for quartz. Ar was found to be preferentially released over Kr and Xe which were believed to be stored in the mineral lattice; up to 88% of the lattice-hosted noble gases were released by prolonged crushing. For obtaining Br/Cl, I/Cl, and $^{40}Ar/^{39}Ar$ age systematics, longer crushing times were found to be an effective method [27].

The relationship between paleocrustal fluids and contemporary groundwaters was investigated based on noble gas ratios of $^{40}Ar/^{36}Ar$, $^{3}He/^{4}He$, $^{40}Ar/^{4}He$ in quartz, and fluorite from the North Pennines ore field (England) [69]. Results indicated the fluid inclusions were characterized by air-saturated water patterns with partly unfractionated atmospheric gases in minerals that had precipitated under atmospheric conditions. Minerals of the North Pennines ore field were identified as crustal He based on $^{3}He/^{4}He$ ratios, while crustal radiogenic production of ^{40}Ar resulted in elevated $^{40}Ar/^{36}Ar$ ratios above atmospheric. While up to five crushes were applied to olivine, the main release of ^{4}He and ^{40}Ar occurred at the first crush and then decreased with further crush steps. At the same time, an increase in the $^{40}Ar/^{36}Ar$ ratio with each crush step was interpreted as a contribution of atmospheric argon from secondary inclusions.

Finally, although a summary of noble gas characteristics in different layers of the crust and mantle would be very interesting, this was beyond the scope of the current review of crushing techniques. Note that a summary of noble gas isotopes in different rock types of mantle or crustal origin is given in Figures 1 and 2. Readers may find further information on noble gas isotope patterns in mantle and crust rocks in [150–152].

6. Summary and Conclusions

This review of crushing techniques identified three main ways of ultrahigh vacuum crushing systems: magnetic crusher, shaking- or milling-type crusher, and piston-type crusher. Several modifications of these three crusher types were reported and involved automatic handling, the use of multiple crushing containers, and adjustable pressure capabilities. Piston-style crushers were shown to be applicable to most if not all geoscientific studies reviewed, while magnetic crushers were primarily used on crustal rock for the purpose of mantle studies. A wide range of noble gas isotopes has been analysed following mineral crushing, with the selection of isotopes not limited by the crushing technique but rather depending on the research question at hand and the available analytical measurement technique. The crushing techniques reviewed had been used for a wide range of geoscientific applications, including the characterization of ore evolvement, mantle-crustal identification, paleoclimate estimations, characterization of surface and erosion processes, and the identification of extraterrestrial rocks or deep fluids in Earth's crust.

An important limitation of all crushing techniques reviewed is their inability to separate inclusions embedded in fracture infillings from inclusions within the mineral matrix. For example, crushing of quartz grains typically releases noble gases from both fluid inclusions of different generations (melt inclusions, primary and secondary inclusions) and to a minor degree the matrix. Unless one can separate those, any mineral/rock age determination will be a based on a mixture of those three sources of noble gases.

This review has shown that there is a lack of technical details of crushing conditions before and after the experiments as well as comparisons to reference systems. Intercomparison of results is therefore difficult because every laboratory has an almost unique approach to undertaking crushing experiments which involves particular modifications resulting in custom-made crushing systems. Key recommendations for future studies are (1) undertake laboratory intercomparison studies to evaluate how comparable the data are that have used different crusher types and (2) explore how selectively measuring larger versus smaller fluid inclusions affects the results, which is especially important for crushing as the smallest fluid inclusions are not typically crushed.

Data Availability

Data can be obtained from this link https://data.csiro.au/collection/csiro%3A58349v1.

Conflicts of Interest

The authors declare no conflict of interests for this submission.

Acknowledgments

This study is funded by the Environment Business Unit of CSIRO, Australia's National Science Agency. Open Access funding enabled and organized by the CSIRO 2023.

References

[1] J. Lippmann-Pipke, B. S. Lollar, S. Niedermann et al., "Neon identifies two billion year old fluid component in Kaapvaal Craton," *Chemical Geology*, vol. 283, no. 3-4, pp. 287–296, 2011.

[2] X. F. Li, J. W. Mao, D. H. Wang, F. X. Luo, and T. G. Zhu, "Helium and argon isotope systematics in fluid inclusion of the gold deposits along the Daduhe River, Sichuan Province, West China," in *Mineral Exploration and Sustainable Development, Vols 1 and 2*, pp. 993–996, Millpress Science Publishers, Rotterdam, 2003.

[3] J. W. Mao, R. Kerrich, H. Y. Li, and Y. H. Li, "High 3He/4He ratios in the Wangu gold deposit, Hunan province, China: implications for mantle fluids along the Tanlu deep fault zone," *Geochemical Journal*, vol. 36, no. 3, pp. 197–208, 2002.

[4] J. Mao, Y. Li, R. Goldfarb, Y. He, and K. Zaw, "Fluid inclusion and noble gas studies of the Dongping gold deposit, Hebei Province, China: a mantle connection for mineralization?," *Economic Geology*, vol. 98, no. 3, pp. 517–534, 2003.

[5] R. Shen, Y. Shen, T. Liu, G. Li, and Q. Zeng, "Rare-earth element and noble gas studies of Kuoerzhenkuola gold field, Xinjiang, China: a mantle connection for mineralization," in *Mineral Deposit Research: Meeting the Global Challenge, Vols 1 and 2*, pp. 1335–1338, Springer, Berlin, 2005.

[6] G. Xie, J. Mao, W. Li et al., "Different proportion of mantle-derived noble gases in the Cu-Fe and Fe skarn deposits: He-Ar isotopic constraint in the Edong district, Eastern China," *Ore Geology Reviews*, vol. 72, pp. 343–354, 2016.

[7] D. Chavrit, R. Burgess, H. Sumino et al., "The contribution of hydrothermally altered ocean crust to the mantle halogen and noble gas cycles," *Geochimica et Cosmochimica Acta*, vol. 183, pp. 106–124, 2016.

[8] M. Trieloff, J. Kunz, D. A. Clague, D. Harrison, and C. J. Allègre, "The nature of pristine noble gases in mantle plumes," *Science*, vol. 288, no. 5468, pp. 1036–1038, 2000.

[9] D. V. Bekaert, G. Avice, and B. Marty, "Origin and significance of cosmogenic signatures in vesicles of lunar basalt 15016," *Meteoritics & Planetary Science*, vol. 53, no. 6, pp. 1238–1251, 2018.

[10] B. Marty, S. Kelley, and G. Turner, "Chronology and shock history of the Bencubbin meteorite: a nitrogen, noble gas, and Ar-Ar investigation of silicates, metal and fluid inclusions," *Geochimica et Cosmochimica Acta*, vol. 74, no. 22, pp. 6636–6653, 2010.

[11] R. Hetzel, S. Niedermann, S. Ivy-Ochs et al., "^{21}Ne versus ^{10}Be and ^{26}Al exposure ages of fluvial terraces: the influence of crustal Ne in quartz," *Earth and Planetary Science Letters*, vol. 201, no. 3-4, pp. 575–591, 2002.

[12] E. Ghadiri, N. Vogel, M. S. Brennwald et al., "Noble gas based temperature reconstruction on a Swiss stalagmite from the last glacial-interglacial transition and its comparison with other climate records," *Earth and Planetary Science Letters*, vol. 495, pp. 192–201, 2018.

[13] E. Ghadiri, S. Affolter, M. S. Brennwald et al., "Estimation of temperature - altitude gradients during the Pleistocene-Holocene transition from Swiss stalagmites," *Earth and Planetary Science Letters*, vol. 544, article 116387, 2020.

[14] T. Kluge, T. Marx, D. Scholz, S. Niggemann, A. Mangini, and W. Aeschbach-Hertig, "A new tool for palaeoclimate reconstruction: noble gas temperatures from fluid inclusions in speleothems," *Earth and Planetary Science Letters*, vol. 269, no. 3-4, pp. 408–415, 2008.

[15] T. Kluge, T. Marx, W. Aeschbach-Hertig, C. Spötl, and D. K. Richter, "Noble gas concentrations in fluid inclusions as tracer for the origin of coarse-crystalline cryogenic cave carbonates," *Chemical Geology*, vol. 368, pp. 54–62, 2014.

[16] Y. Scheidegger, R. Kipfer, R. Wieler, S. Badertscher, and M. Leuenberger, "Noble gases in Fluid inclusions in speleothems," in *17th Annual VM Goldschmidt Conference*, vol. 71, no. 15pp. A886–A886, Pergamon-Elsevier Science LTD, 2007.

[17] Y. Scheidegger, H. Baur, M. S. Brennwald, D. Fleitmann, R. Wieler, and R. Kipfer, "Accurate analysis of noble gas concentrations in small water samples and its application to fluid inclusions in stalagmites," *Chemical Geology*, vol. 272, no. 1-4, pp. 31–39, 2010.

[18] Y. Scheidegger, M. S. Brennwald, D. Fleitmann, P.-Y. Jeannin, R. Wieler, and R. Kipfer, "Determination of Holocene cave temperatures from Kr and Xe concentrations in stalagmite fluid inclusions," *Chemical Geology*, vol. 288, no. 1-2, pp. 61–66, 2011.

[19] M. C. Castro, P. Goblet, E. Ledoux, S. Violette, and G. de Marsily, "Noble gases as natural tracers of water circulation in the Paris asin: 2. Calibration of a groundwater flow model using noble gas isotope data," *Water Resources Research*, vol. 34, no. 10, pp. 2467–2483, 1998.

[20] M. C. Castro, A. Jambon, G. de Marsily, and P. Schlosser, "Noble gases as natural tracers of water circulation in the Paris Basin: 1. Measurements and discussion of their origin and mechanisms of vertical transport in the basin," *Water Resources Research*, vol. 34, no. 10, pp. 2443–2466, 1998.

[21] O. Warr, B. Sherwood Lollar, J. Fellowes et al., "Tracing ancient hydrogeological fracture network age and compartmentalisation using noble gases," *Geochimica et Cosmochimica Acta*, vol. 222, pp. 340–362, 2018.

[22] G. Holland and S. Gilfillan, "Application of noble gases to the viability of CO2 storage," in *The Noble Gases as Geochemical Tracers*, P. Burnard, Ed., pp. 177–223, Springer, Berlin Heidelberg, Berlin, Heidelberg, 2013.

[23] P. H. Barry, M. Lawson, W. P. Meurer et al., "Determining fluid migration and isolation times in multiphase crustal domains using noble gases," *Geology*, vol. 45, no. 9, pp. 775–778, 2017.

[24] B. Sherwood Lollar, G. Lacrampe-Couloume, G. F. Slater et al., "Unravelling abiogenic and biogenic sources of

methane in the Earth's deep subsurface," *Chemical Geology*, vol. 226, no. 3-4, pp. 328–339, 2006.

[25] A. M. Van den Kerkhof and U. F. Hein, "Fluid inclusion petrography," *Lithos*, vol. 55, no. 1-4, pp. 27–47, 2001.

[26] M. Trieloff, H. W. Weber, G. Kurat, E. K. Jessberger, and J. Janicke, "Noble gases, their carrier phases, and argon chronology of upper mantle rocks from Zabargad Island, Red Sea," *Geochim Cosmochim Acta*, vol. 61, no. 23, pp. 5065–5088, 1997.

[27] M. A. Kendrick and D. Phillips, "New constraints on the release of noble gases during *in vacuo* crushing and application to scapolite Br -Cl-I and $^{40}Ar/^{39}Ar$ age determinations," *Geochimica et Cosmochimica Acta*, vol. 73, no. 19, pp. 5673–5692, 2009.

[28] F. Horton, K. Farley, and M. Jackson, "Helium distributions in ocean island basalt olivines revealed by X-ray computed tomography and single-grain crushing experiments," *Geochimica et Cosmochimica Acta*, vol. 244, pp. 467–477, 2019.

[29] R.-Z. Hu, P. G. Burnard, X.-W. Bi et al., "Helium and argon isotope geochemistry of alkaline intrusion-associated gold and copper deposits along the Red River-Jinshajiang fault belt, SW China," *Chemical Geology*, vol. 203, no. 3-4, pp. 305–317, 2004.

[30] M. Kendrick, R. Burgess, R. Pattrick, and G. Turner, "Halogen and Ar-Ar age determinations of inclusions within quartz veins from porphyry copper deposits using complementary noble gas extraction techniques," *Chemical Geology*, vol. 177, no. 3-4, pp. 351–370, 2001.

[31] M. A. Kendrick and P. Burnard, "Noble gases and halogens in fluid inclusions: a journey through the Earth's crust," in *The Noble Gases as Geochemical Tracers*, P. Burnard, Ed., pp. 319–369, Springer, Berlin Heidelberg, Berlin, Heidelberg, 2013.

[32] M. A. Kendrick, "High precision Cl, Br and I determinations in mineral standards using the noble gas method," *Chemical Geology*, vol. 292-293, pp. 116–126, 2012.

[33] E. F. Baxter, "Diffusion of noble gases in minerals," *Reviews in Mineralogy and Geochemistry*, vol. 72, no. 1, pp. 509–557, 2010.

[34] W. W. Wood, T. F. Kraemer, and P. P. Hearn, "Intragranular diffusion: an important mechanism influencing solute transport in clastic aquifers?," *Science*, vol. 247, no. 4950, pp. 1569–1572, 1990.

[35] E. B. Watson and E. F. Baxter, "Diffusion in solid-earth systems," *Earth and Planetary Science Letters*, vol. 253, no. 3-4, pp. 307–327, 2007.

[36] T. Futagami, M. Ozima, S. Nagal, and Y. Aoki, "Experiments on thermal release of implanted noble gases from minerals and their implications for noble gases in lunar soil grains," *Geochimica et Cosmochimica Acta*, vol. 57, no. 13, pp. 3177–3194, 1993.

[37] D. L. Shuster, K. A. Farley, J. M. Sisterson, and D. S. Burnett, "Quantifying the diffusion kinetics and spatial distributions of radiogenic ^4He in minerals containing proton-induced ^3He," *Earth and Planetary Science Letters*, vol. 217, no. 1-2, pp. 19–32, 2004.

[38] A. J. H. Boerboom and G. Kleyn, "Diffusion coefficients of noble gases in water," *The Journal of Chemical Physics*, vol. 50, no. 3, pp. 1086–1088, 1969.

[39] S. D. Smith, E. Mathouchanh, and D. Mallants, "Quartz-helium method to estimate fluid flow in thick aquitards, Gunnedah Basin, Australia," *Groundwater*, vol. 57, no. 1, pp. 153–165, 2019.

[40] A. H. Manning and A. H. Hofstra, "Noble gas data from goldfield and Tonopah epithermal au-ag deposits, ancestral cascades arc, USA: evidence for a primitive mantle volatile source," *Ore Geology Reviews*, vol. 89, pp. 683–700, 2017.

[41] M. Moreira, J. Kunz, and C. Allègre, "Rare gas systematics in popping rock: isotopic and elemental compositions in the upper mantle," *Science*, vol. 279, no. 5354, pp. 1178–1181, 1998.

[42] G. Holland, B. S. Lollar, L. Li, G. Lacrampe-Couloume, G. Slater, and C. Ballentine, "Deep fracture fluids isolated in the crust since the Precambrian era," *Nature*, vol. 497, no. 7449, pp. 357–360, 2013.

[43] F. M. Stuart, P. G. Burnard, R. P. Taylor, and G. Turner, "Resolving mantle and crustal contributions to ancient hydrothermal fluids: He Ar isotopes in fluid inclusions from Dae Hwa W Mo mineralisation, South Korea," *Geochimica et Cosmochimica Acta*, vol. 59, no. 22, pp. 4663–4673, 1995.

[44] F. Stuart, G. Turner, and R. Taylor, "He–Ar isotope systematics of fluid inclusions: resolving mantle and crustal contributions to hydrothermal fluids," *Noble Gas Geochemistry Cosmochemistry*, J. Matsuda, Ed., pp. 261–277, 1994.

[45] M. Trieloff, M. Falter, A. I. Buikin, E. V. Korochantseva, E. K. Jessberger, and R. Altherr, "Argon isotope fractionation induced by stepwise heating," *Geochimica et Cosmochimica Acta*, vol. 69, no. 5, pp. 1253–1264, 2005.

[46] A. Jambon, H. W. Weber, and F. Begemann, "Helium and argon from an Atlantic MORB glass: concentration, distribution and isotopic composition," *Earth and Planetary Science Letters*, vol. 73, no. 2-4, pp. 255–268, 1985.

[47] I. N. Tolstikhin, A. B. Verchovsky, I. L. Kamensky et al., "Amphibole: a major carrier of helium isotopes in crustal rocks," *Chemical Geology*, vol. 444, pp. 187–198, 2016.

[48] D. W. Graham, P. J. Michael, and K. H. Rubin, "An investigation of mid-ocean ridge degassing using He, CO_2, and $\delta^{13}C$ variations during the 2005-06 eruption at $9^{\circ}50'N$ on the East Pacific Rise," *Earth and Planetary Science Letters*, vol. 504, pp. 84–93, 2018.

[49] M. Pujol, B. Marty, and R. Burgess, "Chondritic-like xenon trapped in Archean rocks: a possible signature of the ancient atmosphere," *Earth and Planetary Science Letters*, vol. 308, no. 3-4, pp. 298–306, 2011.

[50] T. W. Trull and M. D. Kurz, "Experimental measurements of ^3He and ^4He mobility in olivine and clinopyroxene at magmatic temperatures," *Geochimica et Cosmochimica Acta*, vol. 57, no. 6, pp. 1313–1324, 1993.

[51] M. D. Kurz, W. J. Jenkins, J. G. Schilling, and S. R. Hart, "Helium isotopic variations in the mantle beneath the Central North Atlantic Ocean," *Earth and Planetary Science Letters*, vol. 58, no. 1, pp. 1–14, 1982.

[52] M. D. Kurz, W. J. Jenkins, S. R. Hart, and D. Clague, "Helium isotopic variations in volcanic rocks from Loihi Seamount and the Island of Hawaii," *Earth and Planetary Science Letters*, vol. 66, pp. 388–406, 1983.

[53] S. Kelley, G. Turner, A. W. Butterfield, and T. J. Shepherd, "The source and significance of argon isotopes in fluid inclusions from areas of mineralization," *Earth and Planetary Science Letters*, vol. 79, no. 3-4, pp. 303–318, 1986.

[54] D. B. Patterson, K. A. Farley, and B. I. A. McInnes, "Helium isotopic composition of the Tabar-Lihir-Tanga-Feni island

arc, Papua New Guinea," *Geochimica et Cosmochimica Acta*, vol. 61, no. 12, pp. 2485–2496, 1997.

[55] R. J. Bodnar, "Introduction to fluid inclusions," in *Fluid inclusions: analysis and interpretation*, I. Samson, A. Anderson, and D. Marshall, Eds., vol. 32, pp. 1–8, Mineralogical Association of Canada: Short Course, 2003.

[56] H. W. Green and S. V. Radcliffe, "Fluid precipitates in rocks from the Earth's mantle," *GSA Bulletin*, vol. 86, no. 6, pp. 846–852, 1975.

[57] I. P. L. GeotrackJohn Parnell Geofluids Research Group, "Fluid inclusion analysis, extracted from short course notes on fluid inclusion microthermometry," University of Aberdeen: Geotrack international PTY. LTD, 2012.

[58] G. Czuppon, R. R. Ramsay, I. Ozgenc et al., "Stable (H, O, C) and noble-gas (He and Ar) isotopic compositions from calcite and fluorite in the Speewah dome, Kimberley Region, Western Australia: implications for the conditions of crystallization and evidence for the influence of crustal-mantle fluid mixing," *Mineralogy and Petrology*, vol. 108, no. 6, pp. 759–775, 2014.

[59] J. Hopp, W. H. Schwarz, M. Trieloff, H. P. Meyer, M. Hanel, and R. Altherr, "Noble gas composition and 40Ar/39Ar age in eclogites from the main hole of the Chinese continental scientific drilling project," *Contributions to Mineralogy and Petrology*, vol. 171, no. 10, 2016.

[60] G. Magro, G. Ruggieri, G. Gianelli, S. Bellani, and G. Scandiffio, "Helium isotopes in paleofluids and present-day fluids of the Larderello geothermal field: constraints on the heat source," *Journal of Geophysical Research: Solid Earth*, vol. 108, no. B1, pp. ECV 3-1–ECV 3-12, 2003.

[61] A. L. Rizzo, I. T. Uysal, H. Mutlu et al., "Geochemistry of fluid inclusions in travertines from western and northern Turkey: inferences on the role of active faults in fluids circulation," *Geochemistry, Geophysics, Geosystems*, vol. 20, no. 11, pp. 5473–5498, 2019.

[62] Y. C. Liu, M. A. Kendrick, Z. Q. Hou et al., "Hydrothermal fluid origins of carbonate-hosted Pb-Zn deposits of the Sanjiang Thrust Belt, Tibet: indications from noble gases and halogens," *Economic Geology*, vol. 112, no. 5, pp. 1247–1268, 2017.

[63] D. Lal, "In situ-produced cosmogenic isotopes in terrestrial rocks," *Annual Review of Earth and Planetary Sciences*, vol. 16, no. 1, pp. 355–388, 1988.

[64] D. Lal, "Cosmic ray labeling of erosion surfaces: _in situ_ nuclide production rates and erosion models," *Earth and Planetary Science Letters*, vol. 104, no. 2-4, pp. 424–439, 1991.

[65] S. Niedermann, "Cosmic-ray-produced noble gases in terrestrial rocks: dating tools for surface processes," *Reviews in Mineralogy and Geochemistry*, vol. 47, no. 1, pp. 731–784, 2002.

[66] M. Ozima and F. A. Podosek, *Noble Gas Geochemistry*, Cambridge University Press, 2002.

[67] R.-Z. Hu, P. G. Burnard, X.-W. Bi et al., "Mantle-derived gaseous components in ore-forming fluids of the Xiangshan uranium deposit, Jiangxi province, China: evidence from He, Ar and C isotopes," *Chemical Geology*, vol. 266, no. 1-2, pp. 86–95, 2009.

[68] M. A. Kendrick, M. Honda, N. H. S. Oliver, and D. Phillips, "The noble gas systematics of late-orogenic H_2O-CO_2 fluids, Mt Isa, Australia," *Geochimica et Cosmochimica Acta*, vol. 75, no. 6, pp. 1428–1450, 2011.

[69] F. M. Stuart and G. Turner, "The abundance and isotopic composition of the noble gases in ancient fluids," *Chemical Geology: Isotope Geoscience*, vol. 101, no. 1-2, pp. 97–109, 1992.

[70] I. Tolstikhin, I. Kamensky, S. Tarakanov et al., "Noble gas isotope sites and mobility in mafic rocks and olivine," *Geochimica et Cosmochimica Acta*, vol. 74, no. 4, pp. 1436–1447, 2010.

[71] O. Eugster, S. Niedermann, C. Thalmann et al., "Noble gases, K, U, Th, and Pb in native gold," *Journal of Geophysical Research: Solid Earth*, vol. 100, no. B12, pp. 24677–24689, 1995.

[72] M. A. Kendrick, R. Burgess, D. Leach, and R. A. D. Pattrick, "Hydrothermal fluid origins in Mississippi Valley-type ore districts: combined noble gas (He, Ar, Kr) and halogen (Cl, Br, I) analysis of fluid inclusions from the Illinois-Kentucky Fluorspar District, viburnum trend, and Tri-State Districts, Midcontinent United States," *Economic Geology*, vol. 97, no. 3, pp. 453–469, 2002.

[73] M. A. Kendrick, R. Burgess, R. A. D. Pattrick, and G. Turner, "Hydrothermal fluid origins in a fluorite-rich Mississippi Valley-type district: combined noble gas (He, Ar, Kr) and halogen (cl, Br, I) analysis of fluid inclusions from the South Pennine ore field, United Kingdom," *Economic Geology and the Bulletin of the Society of Economic Geologists*, vol. 97, no. 3, pp. 435–451, 2002.

[74] M. A. Kendrick, D. Phillips, M. Wallace, and J. M. Miller, "Halogens and noble gases in sedimentary formation waters and Zn-Pb deposits: a case study from the Lennard Shelf, Australia," *Applied Geochemistry*, vol. 26, no. 12, pp. 2089–2100, 2011.

[75] T. Pettke, R. Frei, J. D. Kramers, and I. M. Villa, "Isotope systematics in vein gold from Brusson, Val d'Ayas (NW Italy) 3. (U \+ Th)He and KAr in native Au and its fluid inclusions," *Chemical Geology*, vol. 135, no. 3-4, pp. 173–187, 1997.

[76] G. Turner and M. P. Bannon, "Argon isotope geochemistry of inclusion fluids from granite-associated mineral veins in southwest and northeast England," *Geochimica et Cosmochimica Acta*, vol. 56, no. 1, pp. 227–243, 1992.

[77] A. I. Buikin, Y. A. Nevinnyi, A. I. Kamaleeva, V. S. Sevast'yanov, and O. V. Kuznetsova, "Equipment and newly developed methodological approaches for isotopic-geochemical studying fluid phases in rocks and minerals," *Geochemistry International*, vol. 55, no. 1, pp. 1–8, 2017.

[78] A. I. Buikin, A. I. Kamaleeva, and N. A. Migdisova, "Prospects of the method of stepwise crushing as a source of information on the fluid phase of rocks and minerals," *Petrology*, vol. 24, no. 3, pp. 303–313, 2016.

[79] T. Staudacher, P. Sarda, and C. J. Allègre, "Noble gas systematics of Reunion Island, Indian Ocean," *Chemical Geology*, vol. 89, no. 1-2, pp. 1–17, 1990.

[80] A. I. Buikin, I. P. Solovova, A. B. Verchovsky, L. N. Kogarko, and A. A. Averin, "PVT parameters of fluid inclusions and the C, O, N, and Ar isotopic composition in a garnet lherzolite xenolith from the oasis Jetty, East Antarctica," *Geochemistry International*, vol. 52, no. 10, pp. 805–821, 2014.

[81] J. Hopp, M. Trieloff, and R. Altherr, "Neon isotopes in mantle rocks from the Red Sea region reveal large-scale plume-lithosphere interaction," *Earth and Planetary Science Letters*, vol. 219, no. 1-2, pp. 61–76, 2004.

[82] J. Hopp, M. Trieloff, and R. Altherr, "Noble gas compositions of the lithospheric mantle below the Chyulu Hills volcanic

field, Kenya," *Earth and Planetary Science Letters*, vol. 261, no. 3-4, pp. 635–648, 2007.

[83] M. Trieloff, J. Kunz, and C. J. Allègre, "Noble gas systematics of the Reunion mantle plume source and the origin of primordial noble gases in Earth's mantle," *Earth and Planetary Science Letters*, vol. 200, no. 3-4, pp. 297–313, 2002.

[84] T. Matsumoto, M. Honda, I. McDougall, and S. Y. O'Reilly, "Noble gases in anhydrous lherzolites from the newer volcanics, southeastern Australia: a MORB-like reservoir in the subcontinental mantle," *Geochimica et Cosmochimica Acta*, vol. 62, no. 14, pp. 2521–2533, 1998.

[85] H. Sumino, K. Nagao, and K. Notsu, "Highly sensitive and precise measurement of helium isotopes using a mass spectrometer with double collector system," *Journal of the Mass Spectrometry Society of Japan*, vol. 49, no. 2, pp. 61–68, 2001.

[86] P. Scarsi, "Fractional extraction of helium by crushing of olivine and clinopyroxene phenocrysts: effects on the $^3He/^4He$ measured ratio," *Geochimica et Cosmochimica Acta*, vol. 64, no. 21, pp. 3751–3762, 2000.

[87] M. W. Broadley, C. J. Ballentine, D. Chavrit, L. Dallai, and R. Burgess, "Sedimentary halogens and noble gases within Western Antarctic xenoliths: implications of extensive volatile recycling to the sub continental lithospheric mantle," *Geochimica et Cosmochimica Acta*, vol. 176, pp. 139–156, 2016.

[88] S. V. S. Murty, S. Basu, and A. Kumar, "Noble gases in South Indian carbonatites: trapped and in situ components," *Journal of Asian Earth Sciences*, vol. 30, no. 1, pp. 154–169, 2007.

[89] N. R. J. Goodwin, R. Burgess, D. Craw, D. A. H. Teagle, and C. J. Ballentine, "Noble gases fingerprint a metasedimentary fluid source in the Macraes orogenic gold deposit, New Zealand," *Mineralium Deposita*, vol. 52, no. 2, pp. 197–209, 2017.

[90] M. D. Kurz, J. M. Warren, and J. Curtice, "Mantle deformation and noble gases: helium and neon in oceanic mylonites," *Chemical Geology*, vol. 266, no. 1-2, pp. 10–18, 2009.

[91] G. Sapienza, D. R. Hilton, and V. Scribano, "Helium isotopes in peridotite mineral phases from Hyblean plateau xenoliths (South-Eastern Sicily, Italy)," *Chemical Geology*, vol. 219, no. 1-4, pp. 115–129, 2005.

[92] D. W. Graham, B. B. Hanan, C. Hémond, J. Blichert-Toft, and F. Albarède, "Helium isotopic textures in Earth's upper mantle," *Geochemistry, Geophysics, Geosystems*, vol. 15, no. 5, pp. 2048–2074, 2014.

[93] K. Konrad, D. W. Graham, C. R. Thornber, R. A. Duncan, A. J. R. Kent, and A. M. Al-Amri, "Asthenosphere-lithosphere interactions in Western Saudi Arabia: inferences from $^3He/^4He$ in xenoliths and lava flows from Harrat Hutaymah," *Lithos*, vol. 248-251, pp. 339–352, 2016.

[94] T. Matsumoto, M. Honda, I. McDougall, S. Y. O'Reilly, M. Norman, and G. Yaxley, "Noble gases in pyroxenites and metasomatised peridotites from the newer volcanics, southeastern Australia: implications for mantle metasomatism," *Chemical Geology*, vol. 168, no. 1-2, pp. 49–73, 2000.

[95] M. Tantillo, G. Riccobono, and A. Rizzo, *Sistema di frantumazione minerali e rocce (crusher) per la stima delle concentrazioni elementari ed isotopiche dei gas nobili contenuti nelle inclusioni fluide*, INGV (Istituto Nazionale di Geofisica e Vulcanologia, Sezione di Palermo), Rome, 2009.

[96] V. A. Nivin, "Helium and argon isotopes in rocks and minerals of the Lovozero alkaline massif," *Geochemistry International*, vol. 46, no. 5, pp. 482–502, 2008.

[97] M. A. Gannibal, I. N. Tolstikhin, A. B. Verchovsky, V. I. Skiba, V. R. Vetrin, and A. V. Gudkov, "Sites and origin of noble gases in minerals: a case study of amphibole from alkaline granitoids of the Kola Peninsula," *Geochemistry International*, vol. 56, no. 11, pp. 1084–1092, 2018.

[98] A. Correale, A. Paonita, M. Martelli et al., "A two-component mantle source feeding Mt. Etna magmatism: insights from the geochemistry of primitive magmas," *Lithos*, vol. 184-187, pp. 243–258, 2014.

[99] M. E. Gennaro, F. Grassa, M. Martelli, A. Renzulli, and A. L. Rizzo, "Carbon isotope composition of CO_2-rich inclusions in cumulate-forming mantle minerals from Stromboli volcano (Italy)," *Journal of Volcanology and Geothermal Research*, vol. 346, pp. 95–103, 2017.

[100] F. Italiano, G. Yuce, M. Di Bella et al., "Noble gases and rock geochemistry of alkaline intraplate volcanics from the Amik and Ceyhan-Osmaniye areas, SE Turkey," *Chemical Geology*, vol. 469, pp. 34–46, 2017.

[101] A. L. Rizzo, F. Barberi, M. L. Carapezza et al., "New mafic magma refilling a quiescent volcano: evidence from He-Ne-Ar isotopes during the 2011–2012 unrest at Santorini, Greece," *Geochemistry, Geophysics, Geosystems*, vol. 16, no. 3, pp. 798–814, 2015.

[102] M. E. Gennaro, P. Cosenza, G. Riccobono, M. Tantillo, F. Grassa, and A. Rizzo, *Tecnica di estrazione ed analisi della concentrazione e della composizione isotopica dell'anidride carbonica contenuta nelle inclusioni fluide*, INGV, Rome, 2012.

[103] H. Y. He, R. X. Zhu, and J. Saxton, "Noble gas isotopes in corundum and peridotite xenoliths from the eastern North China Craton: implication for comprehensive refertilization of lithospheric mantle," *Physics of the Earth and Planetary Interiors*, vol. 189, no. 3-4, pp. 185–191, 2011.

[104] Z. Yang, S. Zhai, Z. Yu, and F. Su, "Fluid inclusion and He Ar isotope evidence for subsurface phase separation and variable fluid mixing regimes beneath the Yonaguni Knoll IV hydrothermal field, SOT," *Marine Geology*, vol. 441, article 106630, 2021.

[105] A. L. Rizzo, B. Pelorosso, M. Coltorti et al., "Geochemistry of noble gases and CO2 in fluid inclusions from lithospheric mantle beneath Wilcza Góra (Lower Silesia, Southwest Poland)," *Frontiers in Earth Science*, vol. 6, 2018.

[106] M. Martelli, A. L. Rizzo, A. Renzulli, F. Ridolfi, I. Arienzo, and A. Rosciglione, "Noble-gas signature of magmas from a heterogeneous mantle wedge: the case of Stromboli volcano (Aeolian Islands, Italy)," *Chemical Geology*, vol. 368, pp. 39–53, 2014.

[107] M. Martelli, G. Bianchini, L. Beccaluva, and A. Rizzo, "Helium and argon isotopic compositions of mantle xenoliths from Tallante and Calatrava, Spain," *Journal of Volcanology and Geothermal Research*, vol. 200, no. 1-2, pp. 18–26, 2011.

[108] P. M. Nuccio, A. Paonita, A. Rizzo, and A. Rosciglione, "Elemental and isotope covariation of noble gases in mineral phases from Etnean volcanics erupted during 2001-2005, and genetic relation with peripheral gas discharges," *Earth and Planetary Science Letters*, vol. 272, no. 3-4, pp. 683–690, 2008.

[109] A. Correale, M. Martelli, A. Paonita, A. Rizzo, L. Brusca, and V. Scribano, "New evidence of mantle heterogeneity beneath the Hyblean plateau (Southeast Sicily, Italy) as inferred from noble gases and geochemistry of ultramafic xenoliths," *Lithos*, vol. 132-133, pp. 70–81, 2012.

[110] A. Correale, A. Paonita, A. Rizzo, F. Grassa, and M. Martelli, "The carbon-isotope signature of ultramafic xenoliths from the Hyblean Plateau (Southeast Sicily, Italy): evidence of mantle heterogeneity," *Geochemistry, Geophysics, Geosystems*, vol. 16, no. 3, pp. 600–611, 2015.

[111] G. P. Zeng, Y. J. Gong, X. L. Hu, and S. F. Xiong, "Geology, fluid inclusions, and geochemistry of the Zhazixi Sb-W deposit, Hunan, South China," *Ore Geology Reviews*, vol. 91, pp. 1025–1039, 2017.

[112] M. T. Zhu, L. C. Zhang, G. Wu, H. Y. He, and M. L. Cui, "Fluid inclusions and He![single bond](https://sdfestaticassets-us- east-1.sciencedirectassets.com/shared-assets/55/entities/sbnd.gif)Ar isotopes in pyrite from the Yinjiagou deposit in the southern margin of the North China Craton: a mantle connection for poly-metallic mineralization," *Chemical Geology*, vol. 351, pp. 1–14, 2013.

[113] P. Shen, H. D. Pan, and H. P. Zhu, "Two fluid sources and genetic implications for the Hatu gold deposit, Xinjiang, China," *Ore Geology Reviews*, vol. 73, pp. 298–312, 2016.

[114] C. Yang, X. Geng, F. Yang, and Q. Li, "Metallogeny of the Sarsuk polymetallic Au deposit in the Ashele Basin, Altay Orogenic Belt, Xinjiang, NW China: constraints from mineralogy, fluid inclusions, and He-Ar isotopes," *Ore Geology Reviews*, vol. 100, pp. 77–98, 2018.

[115] T. Matsumoto, Y. Chen, and J. I. Matsuda, "Concomitant occurrence of primordial and recycled noble gases in the Earth's mantle," *Earth and Planetary Science Letters*, vol. 185, no. 1-2, pp. 35–47, 2001.

[116] W. Bach and J. Erzinger, "Volatile components in basalts and basaltic glasses from the EPR at 9° 30'N: East Pacific Rise," *Proceedings of the Ocean Drilling Program, Scientific Results*, vol. 142, pp. 23–29, 1995.

[117] E. Jessberger and W. Gentner, "Mass spectrometric analysis of gas inclusions in Muong Nong glass and Libyan desert glass," *Earth and Planetary Science Letters*, vol. 14, no. 2, pp. 221–225, 1972.

[118] G. Avice, B. Marty, and R. Burgess, "The origin and degassing history of the Earth's atmosphere revealed by Archean xenon," *Nature Communications*, vol. 8, no. 1, article 15455, 2017.

[119] G. Avice, B. Marty, R. Burgess et al., "Evolution of atmospheric xenon and other noble gases inferred from Archean topaleoproterozoic rocks," *Geochimica et Cosmochimica Acta*, vol. 232, pp. 82–100, 2018.

[120] L. Zimmerman and B. Marty, "Méthodes d'extraction des gaz rares sous ultravide," *Opérations unitaires. Génie de la réaction chimique*, vol. j6632, 2014.

[121] J. Funkhouser, E. Jessberger, O. Müller, and J. Zähringer, "Active and inter gases in Apollo 12 and Apollo 11 samples released by crushing at room temperature and by heating at low temperatures," *Lunar and Planetary Science Conference Proceeding*, vol. 2, p. 1381, 1971.

[122] M. A. Kendrick, M. G. Jackson, E. H. Hauri, and D. Phillips, "The halogen (F, Cl, Br, I) and H_2O systematics of Samoan lavas: assimilated-seawater, EM2 and high- $^3He/^4He$ components," *Earth and Planetary Science Letters*, vol. 410, pp. 197–209, 2015.

[123] M. A. Kendrick, R. Duncan, and D. Phillips, "Noble gas and halogen constraints on mineralizing fluids of metamorphic versus surficial origin: Mt Isa, Australia," *Chemical Geology*, vol. 235, no. 3-4, pp. 325–351, 2006.

[124] M. A. Kendrick, J. M. Miller, and D. Phillips, "Part II. Evaluation of 40Ar-39Ar quartz ages: implications for fluid inclusion retentivity and determination of initial $^{40}Ar/^{36}Ar$ values in Proterozoic samples," *Geochimica et Cosmochimica Acta*, vol. 70, no. 10, pp. 2562–2576, 2006.

[125] M. A. Kendrick, D. Phillips, and J. M. Miller, "Part I. Decrepitation and degassing behaviour of quartz up to 1560 °C: analysis of noble gases and halogens in complex fluid inclusion assemblages," *Geochimica et Cosmochimica Acta*, vol. 70, no. 10, pp. 2540–2561, 2006.

[126] L. H. Johnson, R. Burgess, G. Turner, H. J. Milledge, and J. W. Harris, "Noble gas and halogen geochemistry of mantle fluids: comparison of African and Canadian diamonds," *Geochimica et Cosmochimica Acta*, vol. 64, no. 4, pp. 717–732, 2000.

[127] R. Hu, P. G. Burnard, G. Turner, and X. Bi, "Helium and Argon isotope systematics in fluid inclusions of Machangqing copper deposit in west Yunnan province, China," *Chemical Geology*, vol. 146, no. 1-2, pp. 55–63, 1998.

[128] P. G. Burnard, F. M. Stuart, G. Turner, and N. Oskarsson, "Air contamination of basaltic magmas: Implications for high3He/4He mantle Ar isotopic composition," *Journal of Geophysical Research Planets*, vol. 99, no. B9, pp. 17709–17715, 1994.

[129] D. G. Zhai, J. J. Liu, H. Y. Zhang, S. Tombros, and A. L. Zhang, "A magmatic-hydrothermal origin for Ag-Pb-Zn vein formation at the Bianjiadayuan deposit, inner Mongolia, NE China: evidences from fluid inclusion, stable (C-H-O) and noble gas isotope studies," *Ore Geology Reviews*, vol. 101, pp. 1–16, 2018.

[130] R. Z. Hu, X. W. Bi, G. H. Jian et al., "Mantle-derived noble gases in ore-forming fluids of the granite-related Yaogangxian tungsten deposit, Southeastern China," *Mineralium Deposita*, vol. 47, no. 6, pp. 623–632, 2012.

[131] Y. Y. Tang, X. W. Bi, M. Fayek et al., "Genesis of the Jinding Zn-Pb deposit, Northwest Yunnan Province, China: constraints from rare earth elements and noble gas isotopes," *Ore Geology Reviews*, vol. 90, pp. 970–986, 2017.

[132] Y. Huang, Z. Wu, Z. Sun et al., "He-Ar isotopes and trace gas compositions of fluid inclusions in massive Sulphides from the Yushui copper-polymetallic deposit, South China: metallogenic implications," *Minerals*, vol. 9, no. 5, p. 258, 2019.

[133] V. Lüders and S. Nidermann, "Helium isotope composition of fluid inclusions hosted in massive sulfides from modern submarine hydrothermal systems," *Economic Geology*, vol. 105, no. 2, pp. 443–449, 2010.

[134] G. L. Li, R. M. Hua, W. L. Zhang et al., "He–Ar isotope composition of pyrite and wolframite in the Tieshanlong tungsten deposit, Jiangxi, China: implications for fluid wvolution," *Resource Geology*, vol. 61, no. 4, pp. 356–366, 2011.

[135] M. D. Kurz and W. J. Jenkins, "The distribution of helium in oceanic basalt glasses," *Earth and Planetary Science Letters*, vol. 53, no. 1, pp. 41–54, 1981.

[136] P. Jean-Baptiste and Y. Fouquet, "Abundance and isotopic composition of helium in hydrothermal sulfides from the East Pacific Rise at 13 °N," *Geochimica et Cosmochimica Acta*, vol. 60, no. 1, pp. 87–93, 1996.

[137] P. G. Burnard, R. Hu, G. Turnder, and X. W. Bi, "Mantle, crustal and atmospheric noble gases in ailaoshan gold deposits, Yunnan Province, China," *Geochimica et Cosmochimica Acta*, vol. 63, no. 10, pp. 1595–1604, 1999.

[138] R. H. Goldstein, "Chapter 2: petrographic analysis of fluid inclusions," in *Fluid Inclusions – Analysis and Interpretation*, I. Samson, A. Anderson, and D. Marshall, Eds., vol. 32, pp. 9–53, Mineralogical Association of Canada:Short Course Series, 2003.

[139] H.-N. Qiu and Y.-D. Jiang, "Sphalerite $^{40}Ar/^{39}Ar$ progressive crushing and stepwise heating techniques," *Earth and Planetary Science Letters*, vol. 256, no. 1-2, pp. 224–232, 2007.

[140] E. Roedder, "Fluid inclusions," in *Encyclopedia of Physical Science and Technology*, R. A. Meyers, Ed., pp. 71–77, Academic Press, San Diego, Third edition, 2003.

[141] X. J. Bai, M. Wang, Y. D. Jiang, and H. N. Qiu, "Direct dating of tin-tungsten mineralization of the Piaotang tungsten deposit, South China, by $^{40}Ar/^{39}Ar$ progressive crushing," *Geochimica et Cosmochimica Acta*, vol. 114, pp. 1–12, 2013.

[142] C. Barker and B. E. Torkelson, "Gas adsorption on crushed quartz and basalt," *Geochimica et Cosmochimica Acta*, vol. 39, no. 2, pp. 212–218, 1975.

[143] F. P. Fanale and W. A. Cannon, "Origin of planetary primordial rare gas: the possible role of adsorption," *Geochimica et Cosmochimica Acta*, vol. 36, no. 3, pp. 319–328, 1972.

[144] H. Sumino, R. Burgess, T. Mizukami, S. R. Wallis, G. Holland, and C. J. Ballentine, "Seawater-derived noble gases and halogens preserved in exhumed mantle wedge peridotite," *Earth and Planetary Science Letters*, vol. 294, no. 1-2, pp. 163–172, 2010.

[145] H. Sumino, L. F. Dobrzhinetskaya, R. Burgess, and H. Kagi, "Deep-mantle-derived noble gases in metamorphic diamonds from the Kokchetav massif, Kazakhstan," *Earth and Planetary Science Letters*, vol. 307, no. 3-4, pp. 439–449, 2011.

[146] A. Correale, M. Martelli, A. Paonita, V. Scribano, and I. Arienzo, "A combined study of noble gases, trace elements, and Sr-Nd isotopes for alkaline and tholeiitic lava from the Hyblean Plateau (Italy)," *Lithos*, vol. 314-315, pp. 59–70, 2018.

[147] H. N. Qiu and J. R. Wijbrans, "The paleozoic metamorphic history of the Central Orogenic Belt of China from $^{40}Ar/^{39}Ar$ geochronology of eclogite garnet fluid inclusions," *Earth and Planetary Science Letters*, vol. 268, no. 3-4, pp. 501–514, 2008.

[148] X. J. Bai, M. Liu, R. G. Hu et al., "Well-constrained mineralization ages by integrated 40Ar/39Ar and U-Pb dating techniques for the Xitian W-Sn polymetallic Deposit, South China," *Economic Geology*, vol. 117, no. 4, pp. 833–852, 2021.

[149] F. Stuart, R. Duckworth, G. Turner, and P. Schofield, "Helium and sulfur isotopes of sulfide minerals from middle valley, northern Juan De Fuca ridge," *Proceedings of the Ocean Drilling Program, Scientific Results*, vol. 139, pp. 388–406, 1994.

[150] I. D. Clark and R. J. Phillips, "Geochemical and $^{3}He/^{4}He$ evidence for mantle and crustal contributions to geothermal fluids in the western Canadian continental margin," *Journal of Volcanology and Geothermal Research*, vol. 104, no. 1-4, pp. 261–276, 2000.

[151] C. Gautheron and M. Moreira, "Helium signature of the subcontinental lithospheric mantle," *Earth and Planetary Science Letters*, vol. 199, no. 1-2, pp. 39–47, 2002.

[152] W. M. White, *Isotope Geochemistry, Chapter 12*, Wiley, 2015.